Smart Materials Research at UAHuntsville

Mark W. Lin, Ph.D.
Associate Professor
Department of Mechanical and Aerospace Engineering
University of Alabama in Huntsville
Huntsville, Alabama

UAHuntsville Materials Science Faculty Research Symposium

December 05, 2012

Outline

- Introduction
- Electrical Time Domain Reflectometry (ETDR) Distributed Strain Sensor
- Impedance-Based Piezoelectric Sensor
- Hybrid Linear/Rotary Actuator
- Shape Memory Alloy (Nitinol) Active Actuator
- FEA Structural Analyses
- Closing Thought

Smart Structures

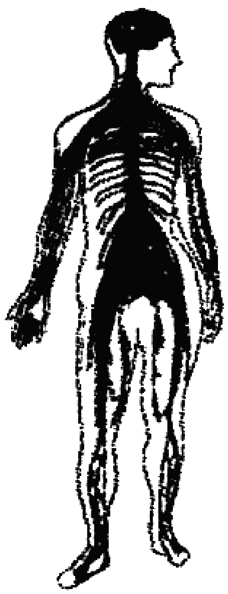

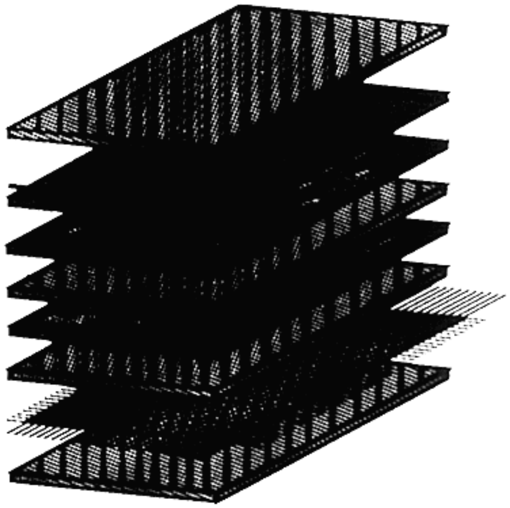

SKELETON	composite/structural materials
MUSCULAR SYSTEM	piezoelectric ceramics, piezoelectric polymers, shape memory alloys
SENSORY SYSTEM	optical fiber sensors, piezoelectric polymer sensors, ETDR distributed strain sensors
MOTOR CONTROL SYSTEM	modern distributed control algorithms

UAH

Engineering Applications

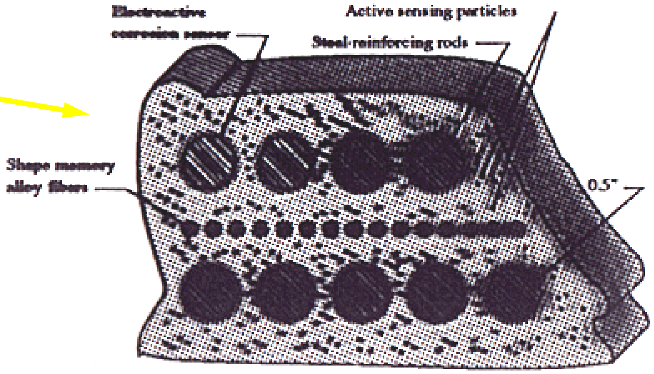

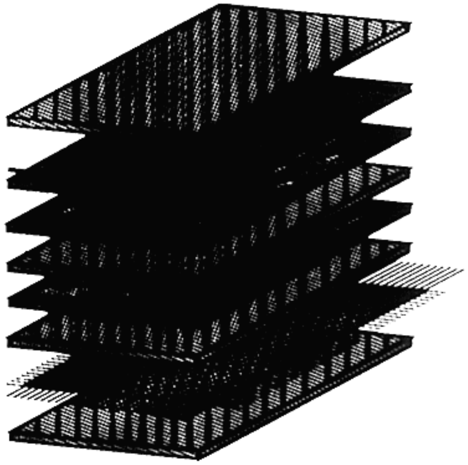

Smart Structures Design Philosophy

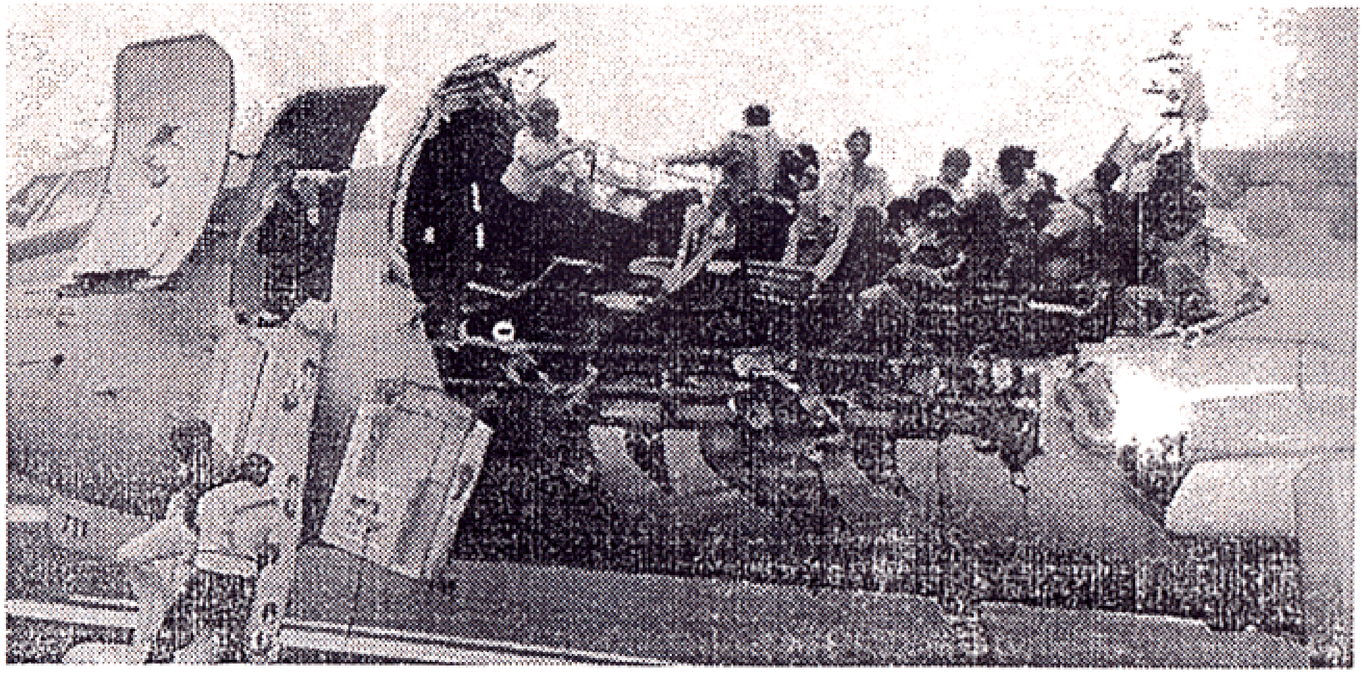

- The material/structural systems can sense a need, can change based upon the need, and can correct a mistake
- Engineers will not have to learn from structural failures, but will be able to learn from the "life experiences" of the structure.

UAH

Discrete vs. Distributed Strain Sensing

Discrete/Point Strain Sensing

- Well-developed sensors currently available, such as strain gages, LVDT displacement sensors, piezoelectric transducers, Eddy current sensor, etc.
- Acquiring data only at the points of interest
- At the location where no sensor is present, direct measurements are not available
- In practice, sensors are strategically placed at critical locations, and a mechanics-based model is used to subsequently approximate the structural response at other locations, if such data are needed

Distributed Strain Sensing

- Capable of measuring the needed data along the sensing line for the entire structure.
- Having a potential to monitor integrity condition of an in-service structure, since structural failure can occur at any location.

Distributed Strain Sensors Currently Being Studied

- Fiber optic sensor using Bragg grating method (quasi distributed)
- Fiber optic sensor using Brillouin scattering method (true distributed, low spatial resolution, >4in)
- Electrical time domain reflectometry (ETDR) strain sensor (true distributed, high spatial resolution, >0.16 in)

UAH

ETDR Distributed Strain Sensing

Principle of Electrical Time Domain Reflectometry (ETDR) Distributed Sensing

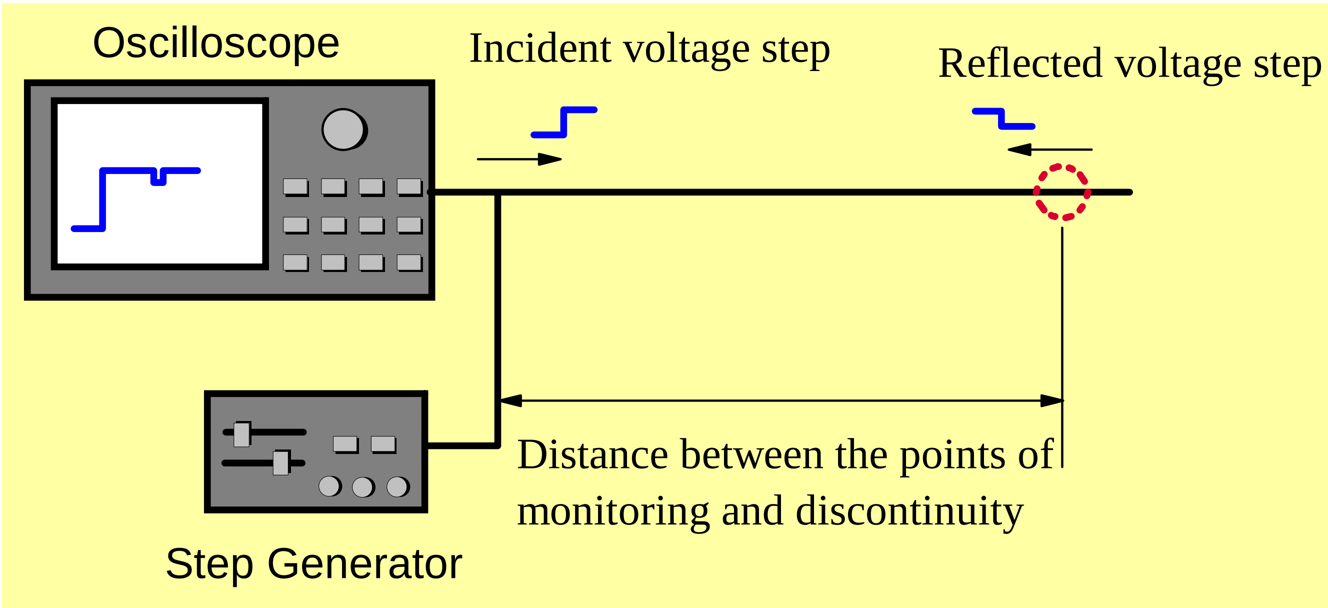

$$Z = [(R + \omega jL) / (G + \omega jC)]^{1/2}$$

***Z*: Characteristic Impedance**
***R*: Resistance**
***L*: Inductance**
***G*: Conductivity**
***C*: Capacitance**

- **Fault Detection along a Power Transmission Coaxial Cable**
- **Signal Integrity Testing in an Electronic Package**

UAH

Distributed Strain Sensing Mechanism

Coaxial Cable

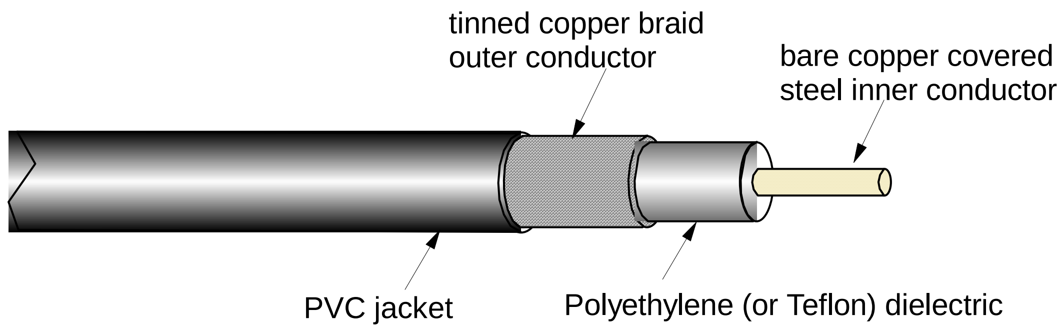

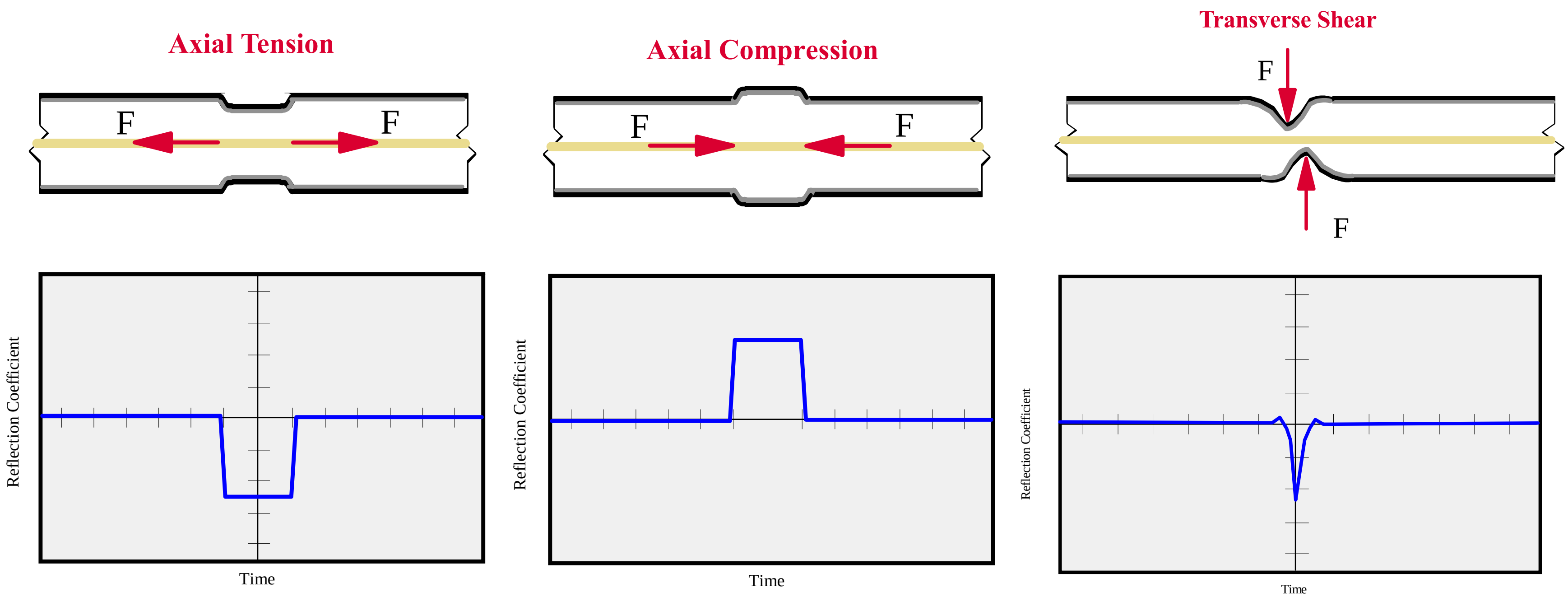

Embedded ETDR Sensor

Strain Measurement

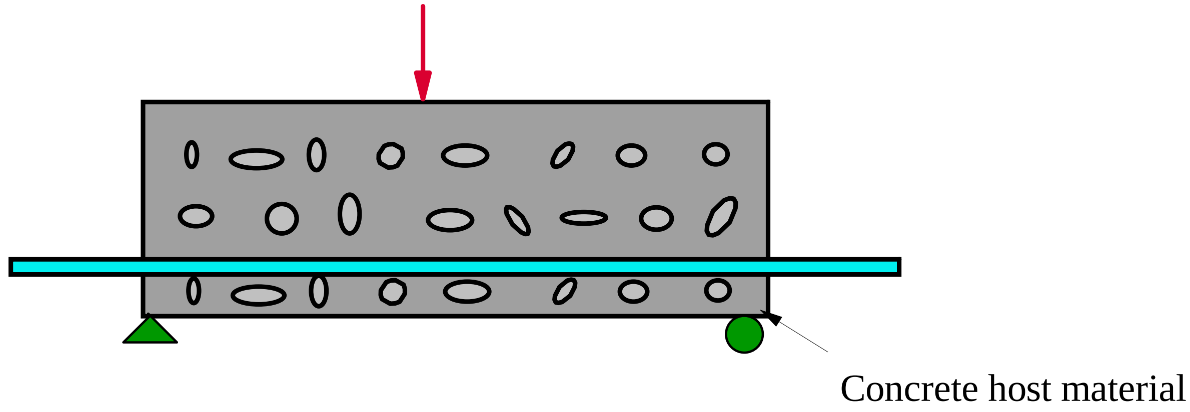

Detection and Measurement of Stress Concentration

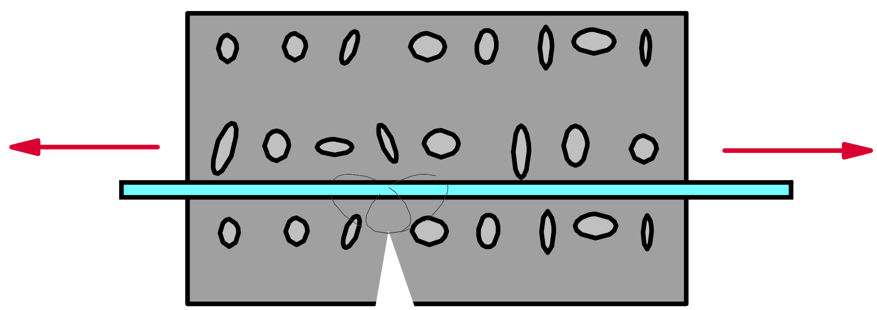

Crack Damage Detection

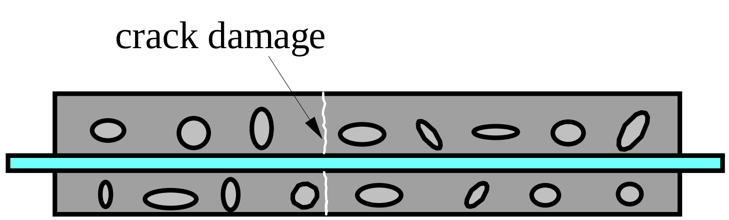

Commercial Coaxial Sensor

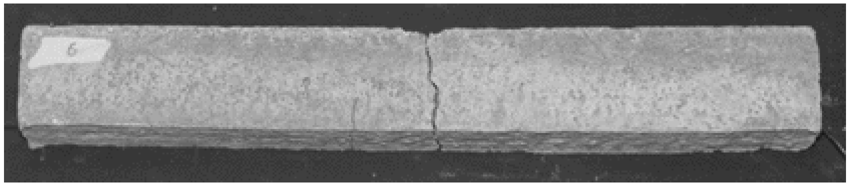

Concrete Beam with Embedded Commercial RG-174 Coaxial Sensor Subjected to 3-Point Bending

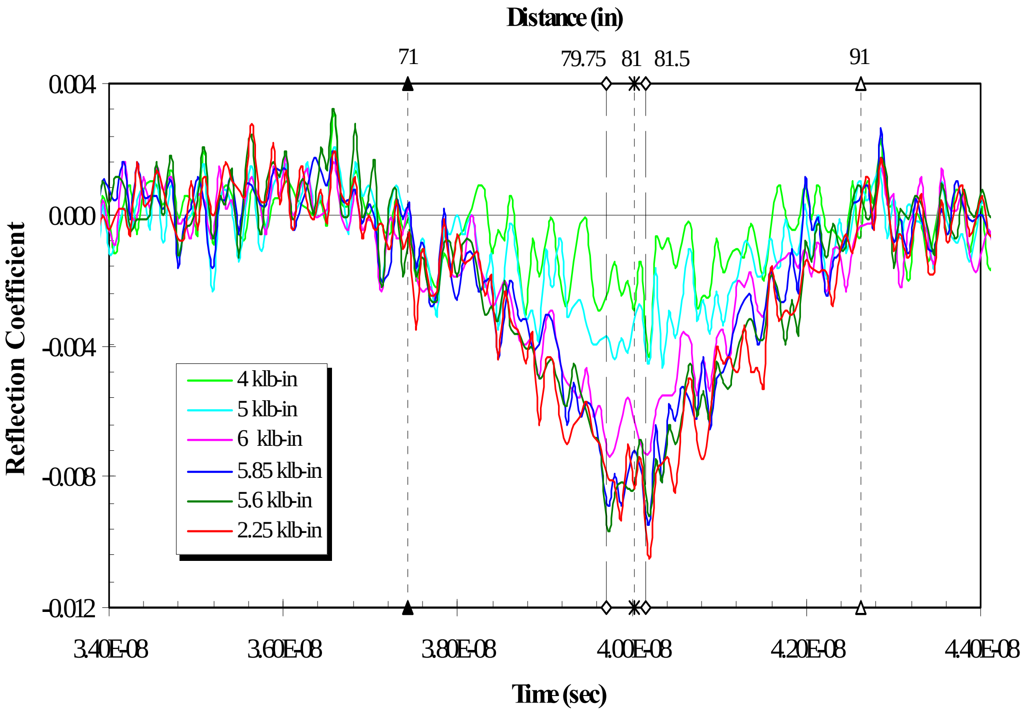

Commercial Coaxial Cable

- Capture Deformation Shape
- Low Signal-to-Noise Ratio

UAH

High Sensitivity ETDR Prototype Sensor

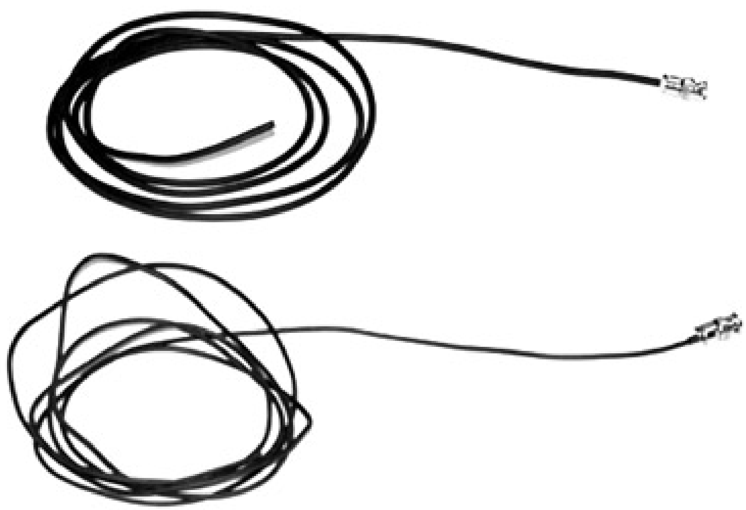

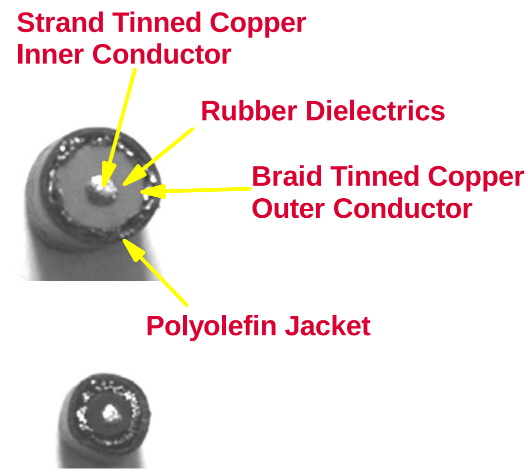

	Outer Diameter of Polyolefin Jacket (in)	Outer Diameter of Outer Conductor (in)	Outer Diameter of Dielectric (in)	Diameter of Inner Conductor (in)	Impedance (Ω)	Dielectric Constant
Large Cable	0.182	0.1606	0.1395	0.0483	40	2.8983
Small Cable	0.138	0.0985	0.0642	0.0303	40	2.7496

Sensitivity Test

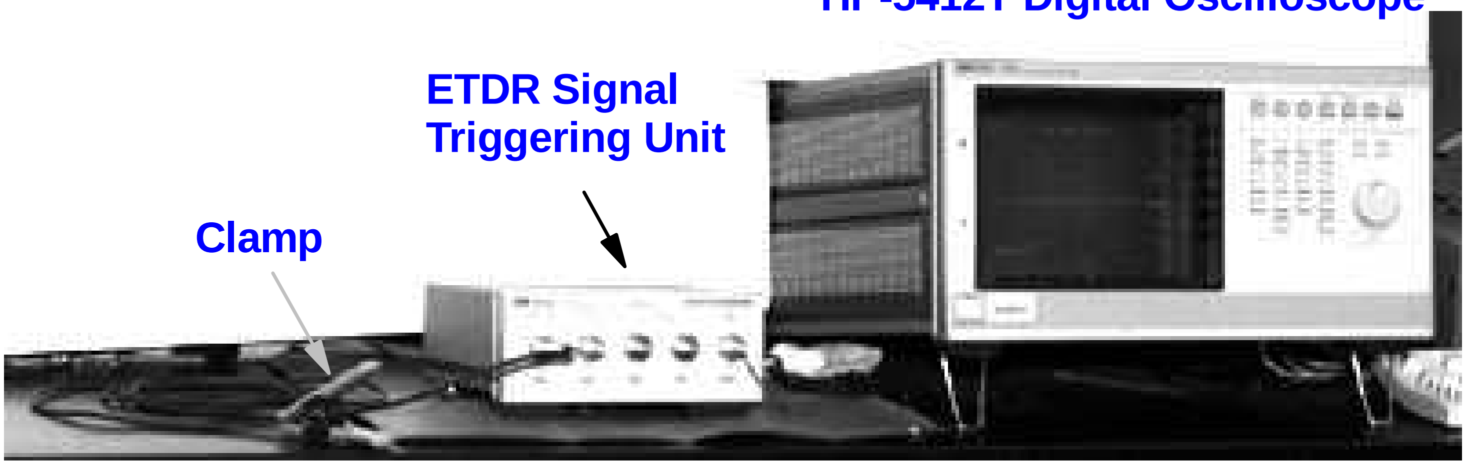

High Sensitivity ETDR Prototype Sensor Subject to a Constant Spring Force of 28 lbs.

Sensitivity Test (Cont.)

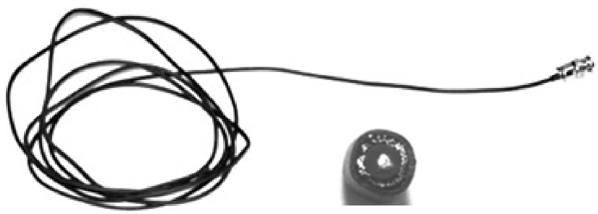

ETDR signal sensitivity response of large prototype cable

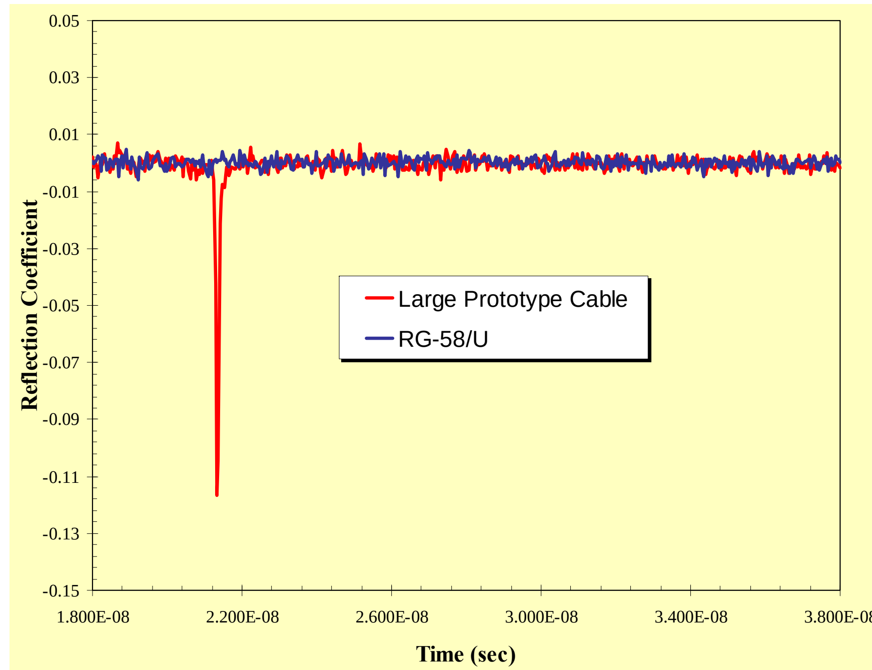

ETDR signal sensitivity response of small prototype cable

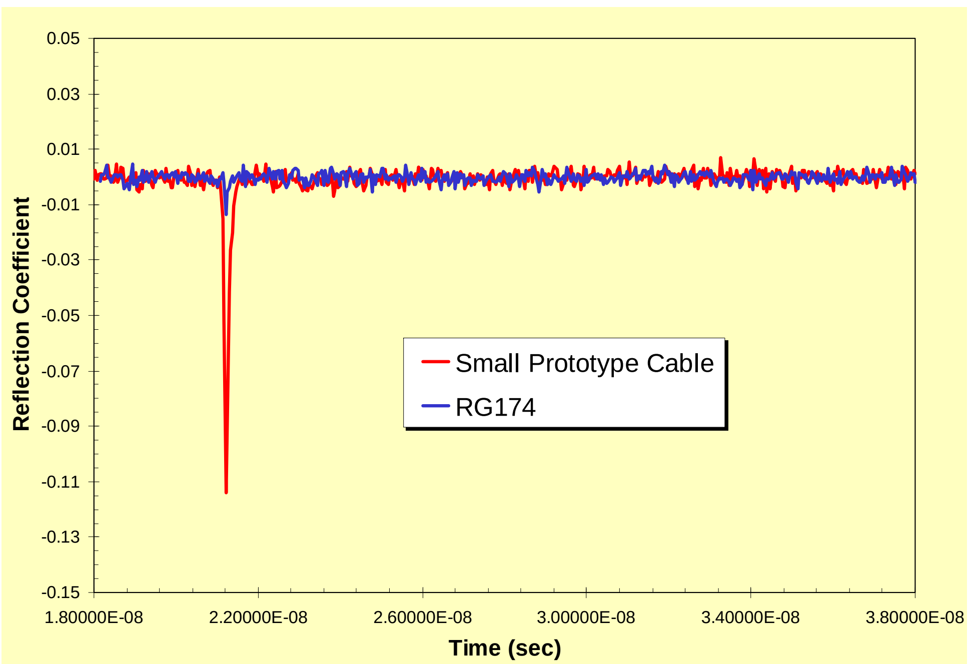

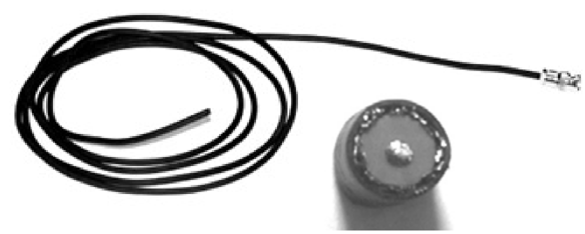

Tension Test

Experimental Setup

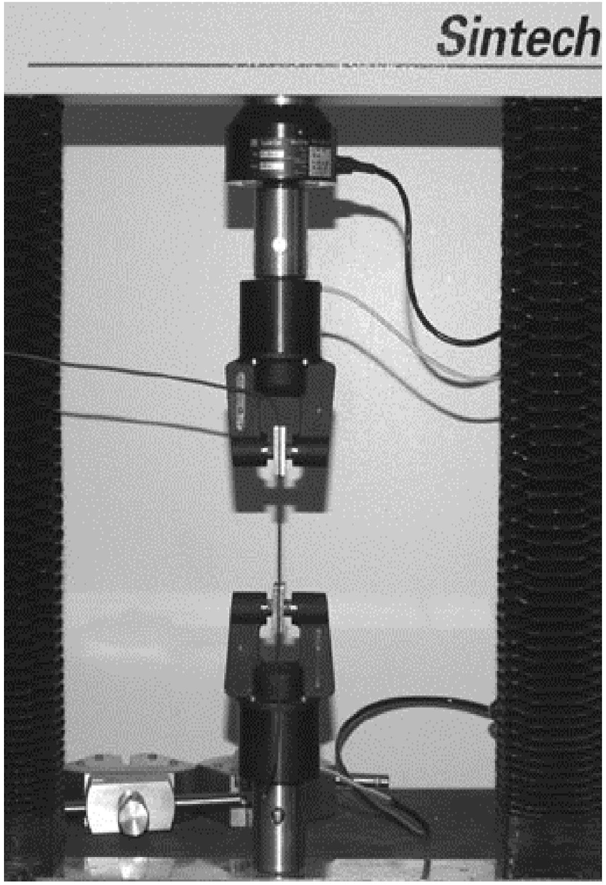

Comparison of ETDR signal response of high sensitivity prototype cable and commercial RG174 cable subject to axial tension

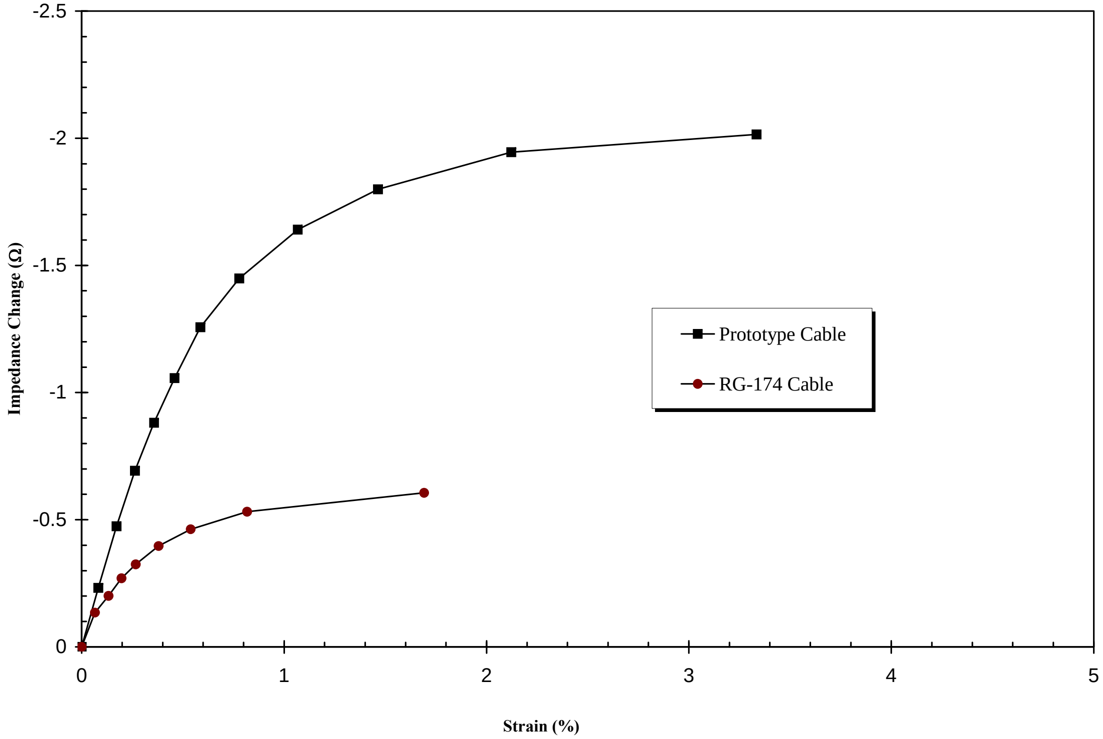

Calibration of ETDR Signal Waveform

Infinite Reflections

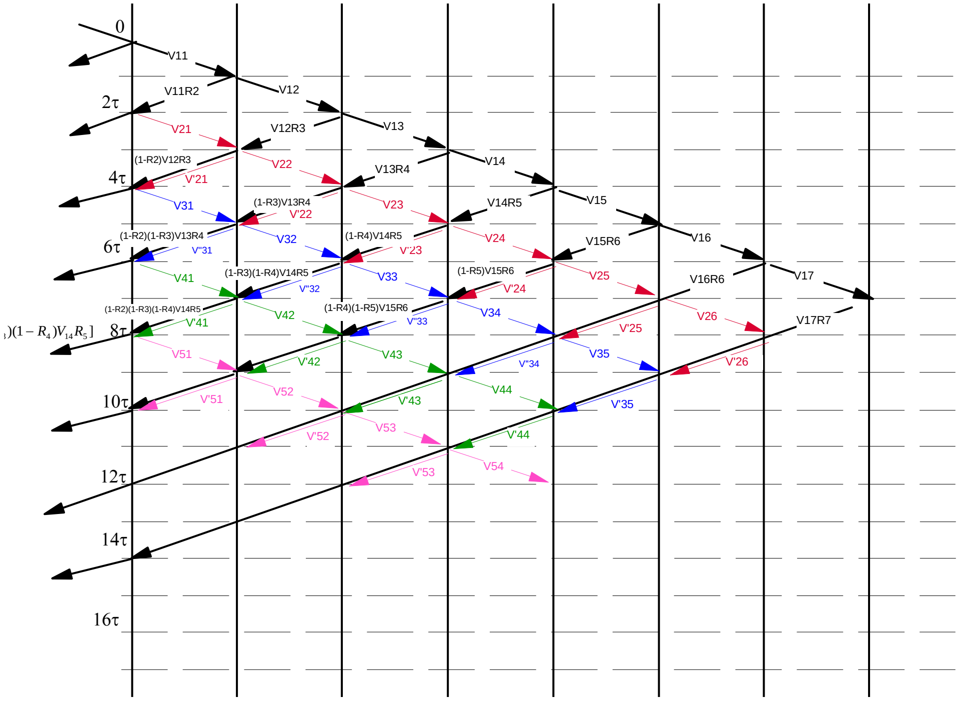

Reflection Coefficient

$$V_{mn} = (1+\rho_n)V_{m(n-1)} + (-\rho_n)[V'_{(m-1)n} + V_{1(n+m-2)}\rho_{(n+m-1)} \prod_{i=n+1}^{n+m-2}(1-\rho_i)]$$

$$V'_{mn} = V_{mn}\rho_{n+1} + (1-\rho_{n+1})V'_{(m-1)(n+1)}$$

$$\Delta V_i = (1-\rho_1)V'_{i-1,1} + V_{1,i-1}\rho_i \prod_{j=1}^{i-1}(1-\rho_j)$$

$$\rho_i = \frac{(\Delta V_i - (1-\rho_1)V'_{i-1,1})}{V_{1,i-1}\cdot \prod_{j=1}^{i-1}(1-\rho_j)}$$

Impedance

$$Z_i = Z_{i-1}\cdot\frac{(1+\rho_i)}{(1-\rho_i)}$$

Bending Response Monitoring of a Concrete Beam

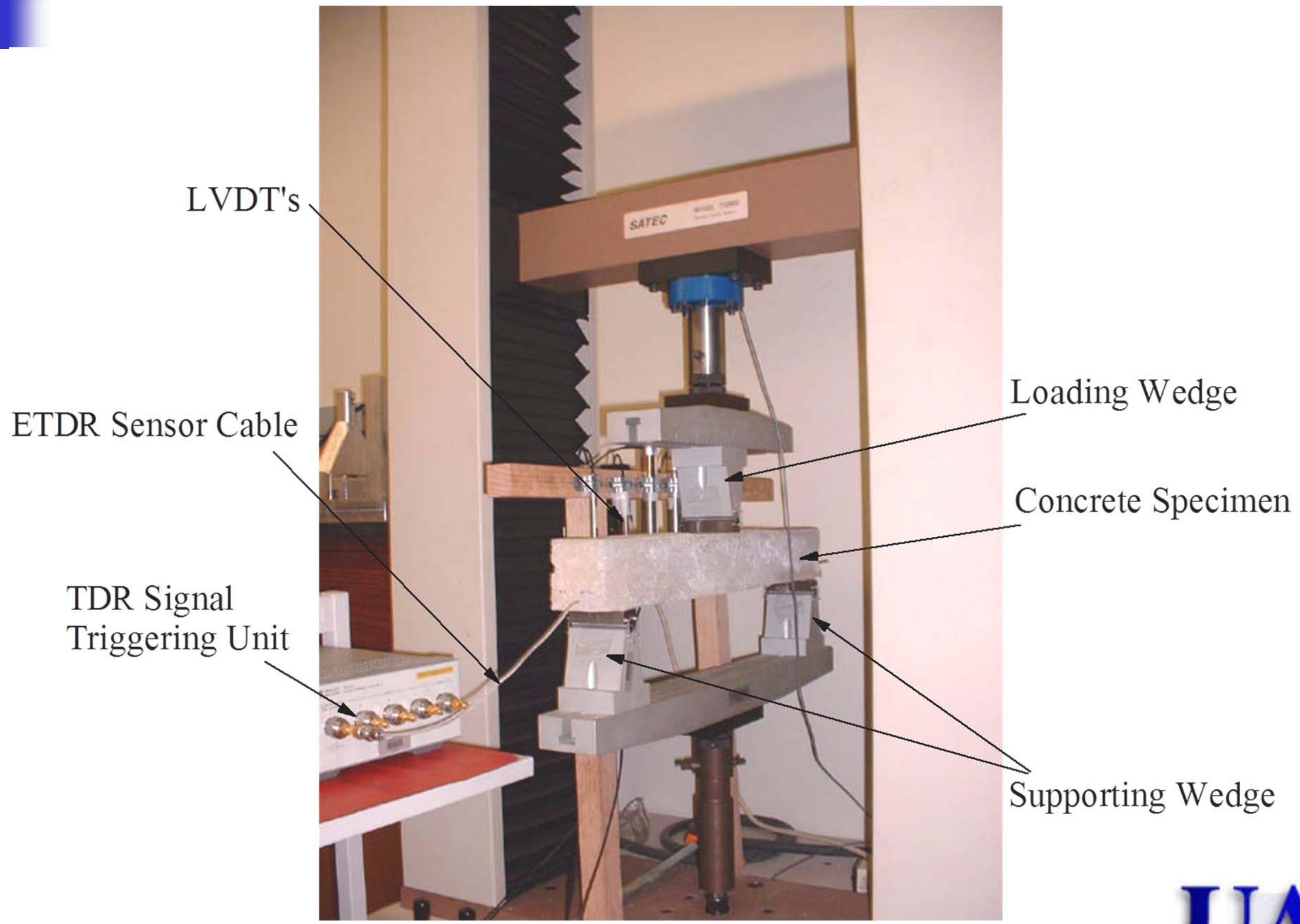

UAH

Bending Response - Results (Cont.)

Deflection Profile of the Beam

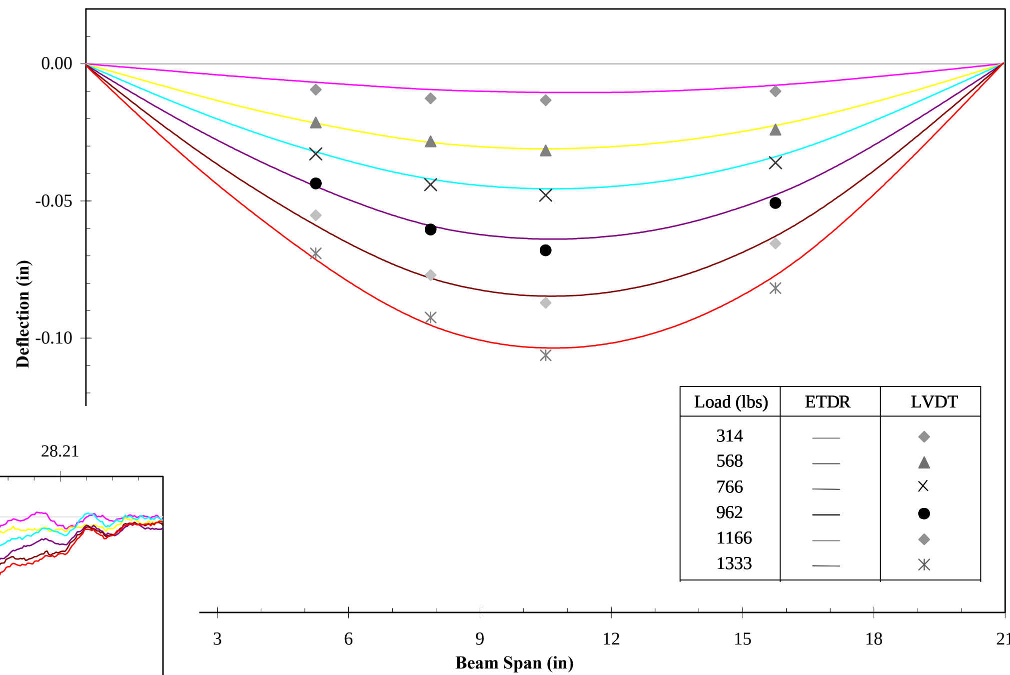

ETDR Signal Waveforms

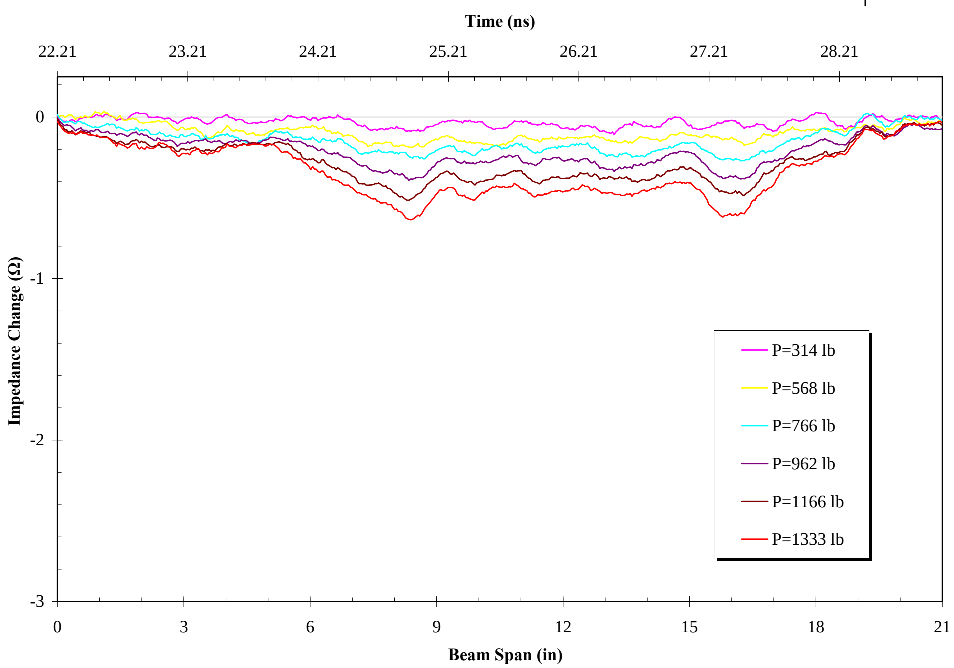

UAH

Damage Detection

ETDR Signal Waveforms

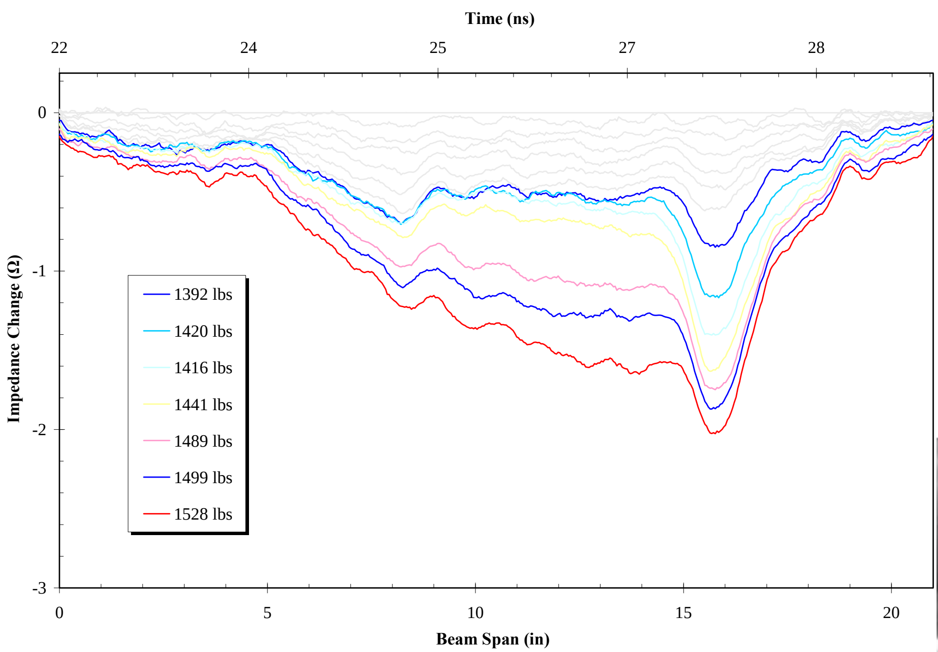

Crack Damages

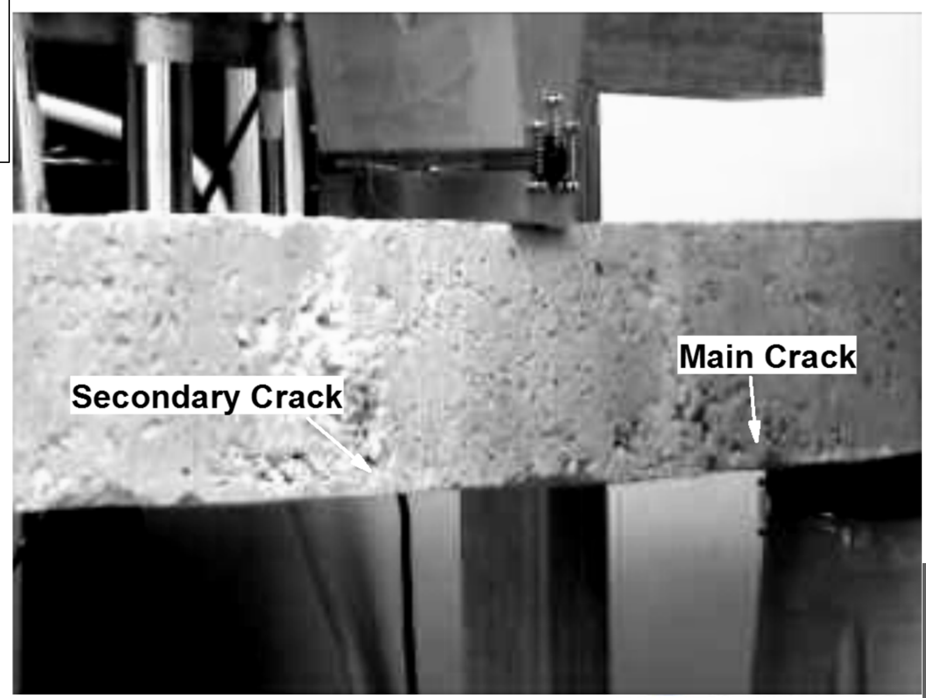

In the Near Future

Field Application

Dam

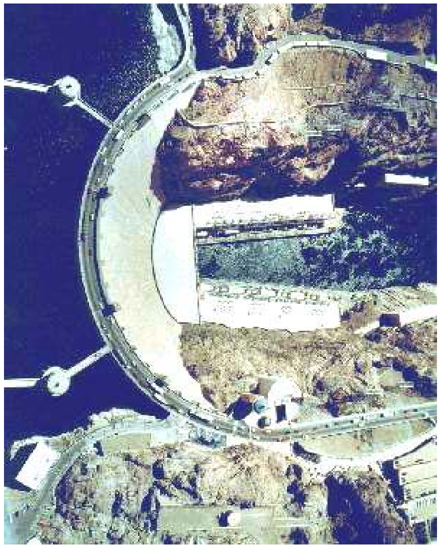

Landslide

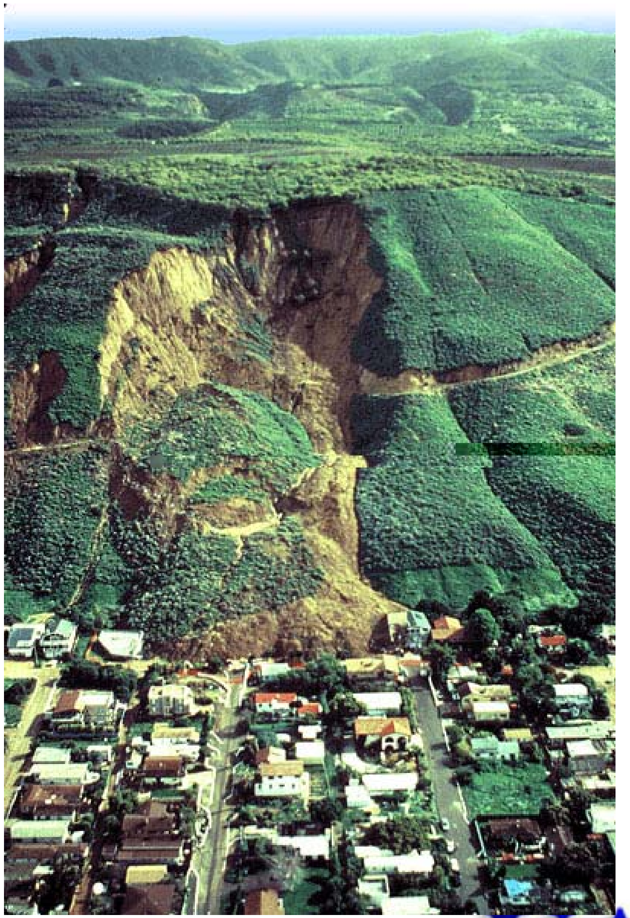

Bridge

Large Flexible Aerospace Structures

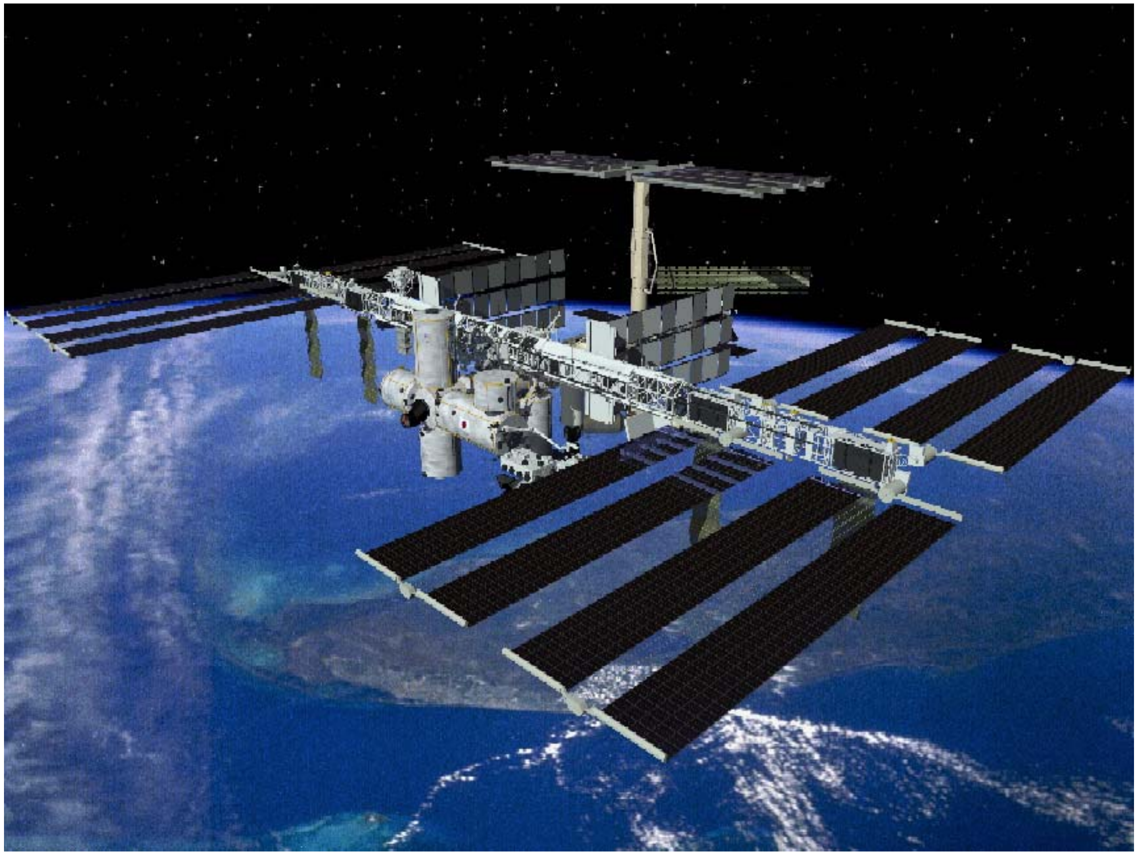

- **Deformation Shape Measurement**
- **Structural Integrity Monitoring**

UAH

Shape Measurement of Large Structure

Experimental Setup

ETDR Signal Triggering Unit

Fixture

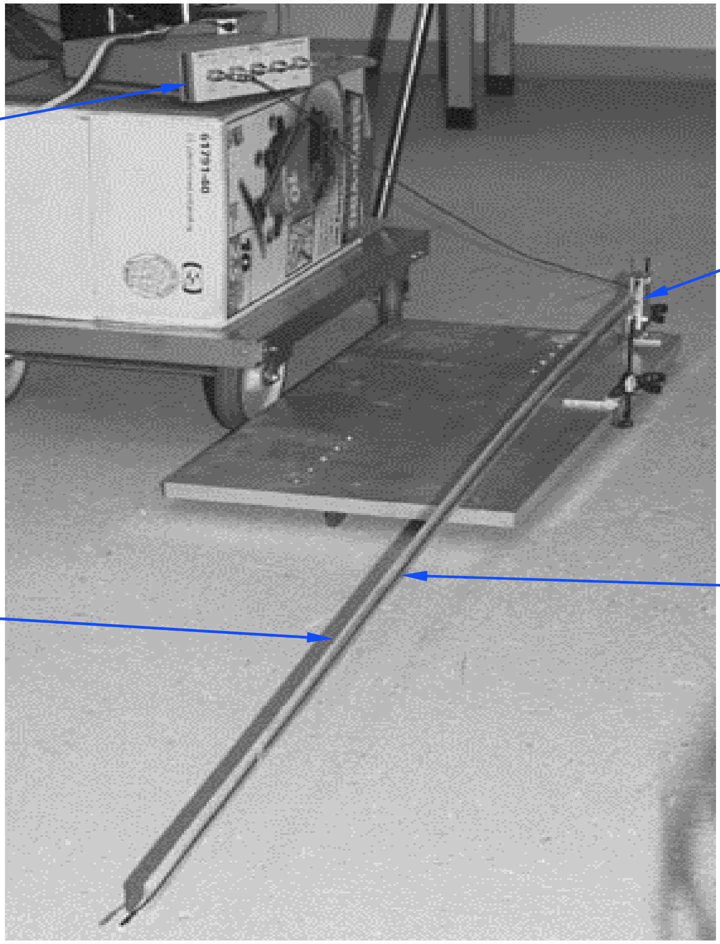

Wooden Beam (1.5x0.2x72 in.) with Surface-Bonded High Sensitivity Prototype Cable

High Sensitivity ETDR Prototype Cable

UAH

Shape Measurement of Large Structure (Cont.)

1st Mode Bending

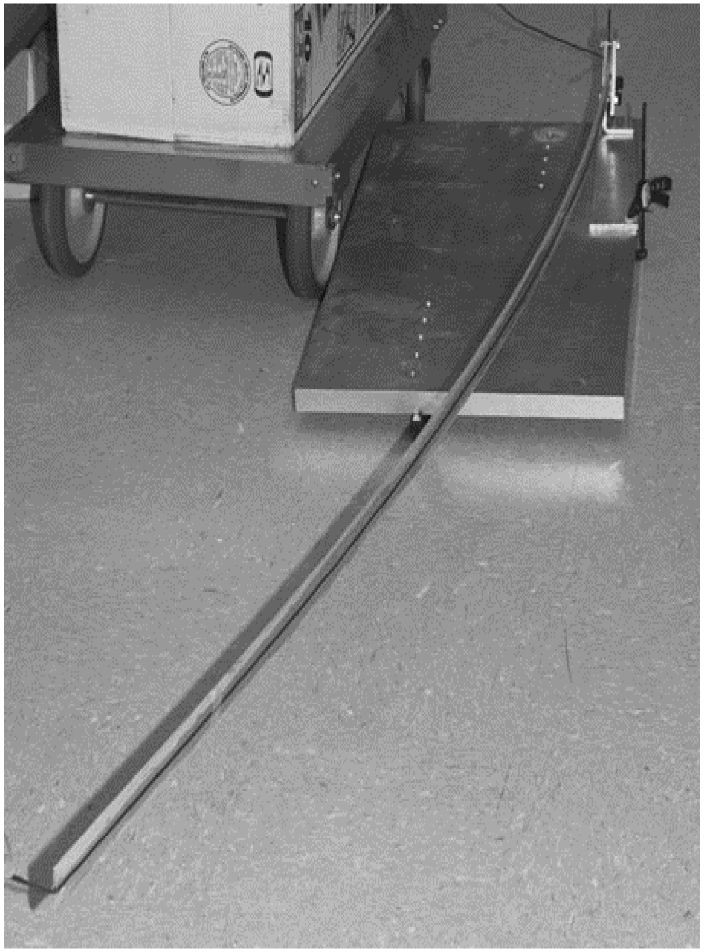

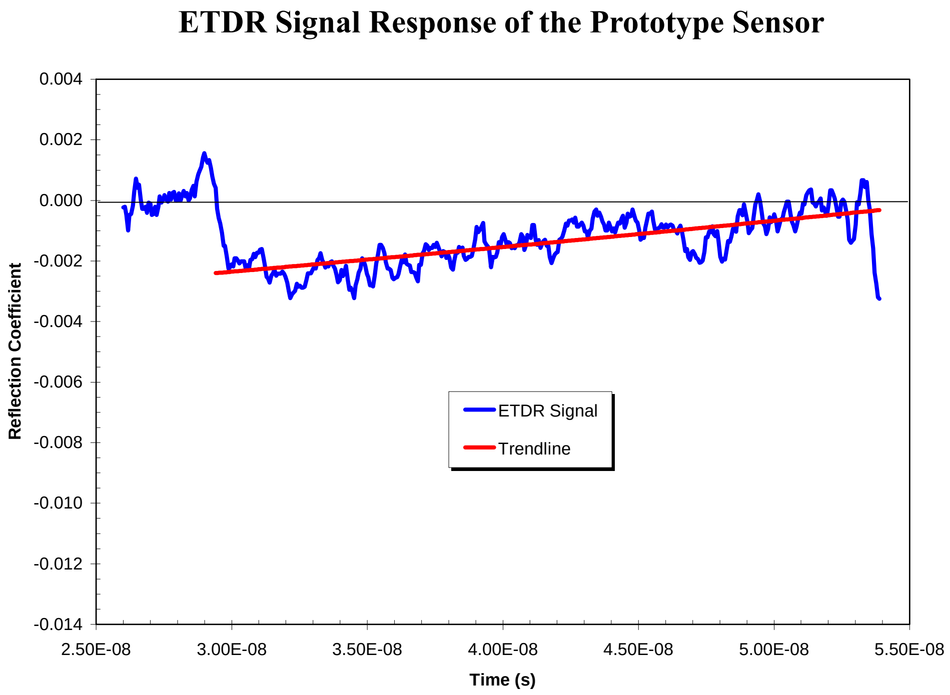

Shape Measurement of Large Structure (Cont.)

2nd Mode Bending

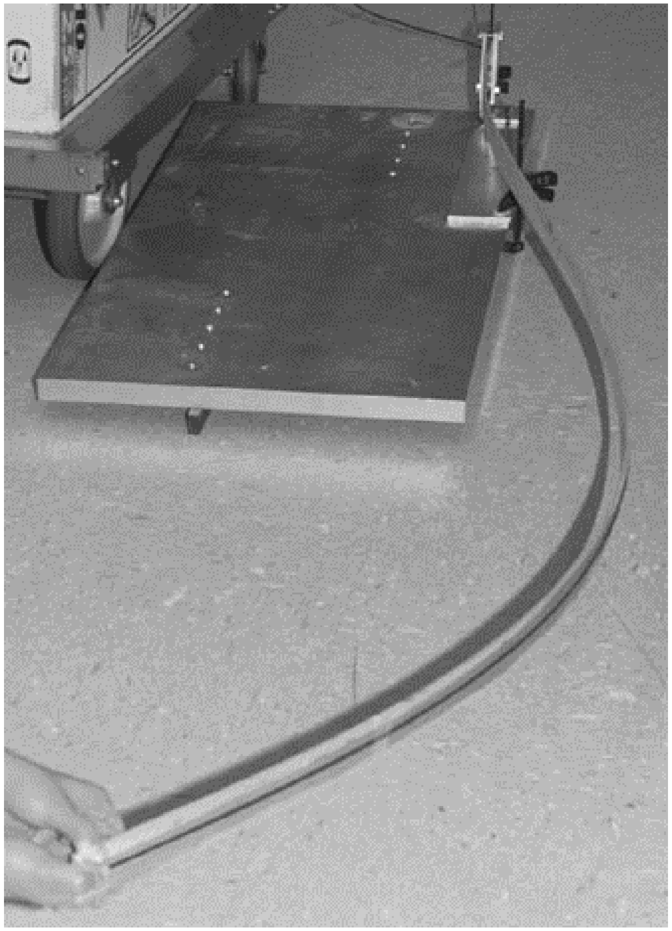

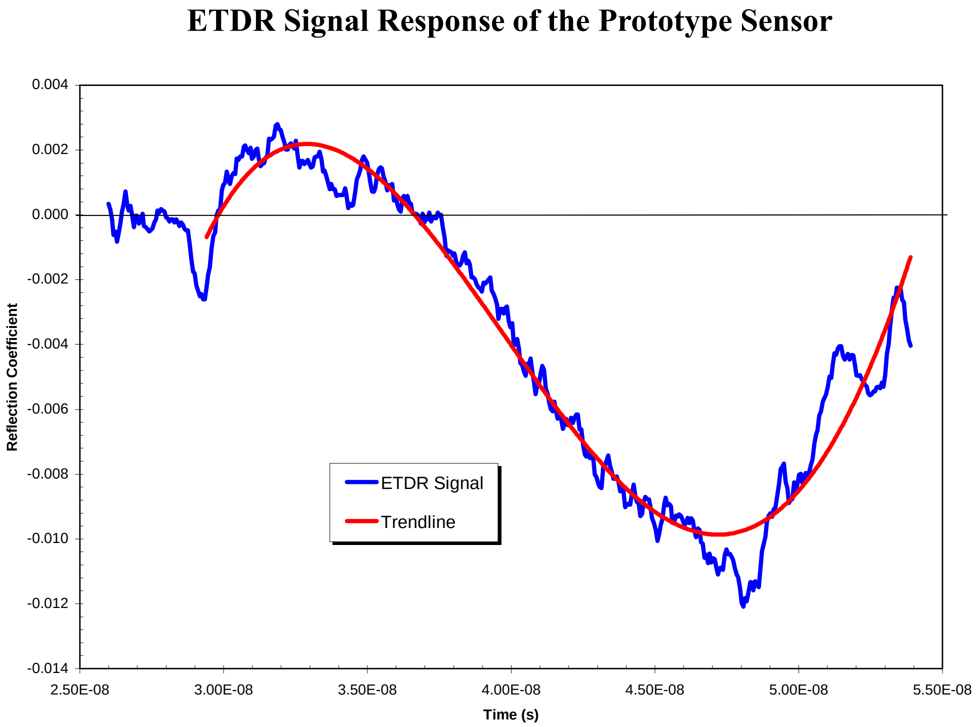

Shape Measurement of Large Structure (Cont.)

1st Mode Reverse Bending

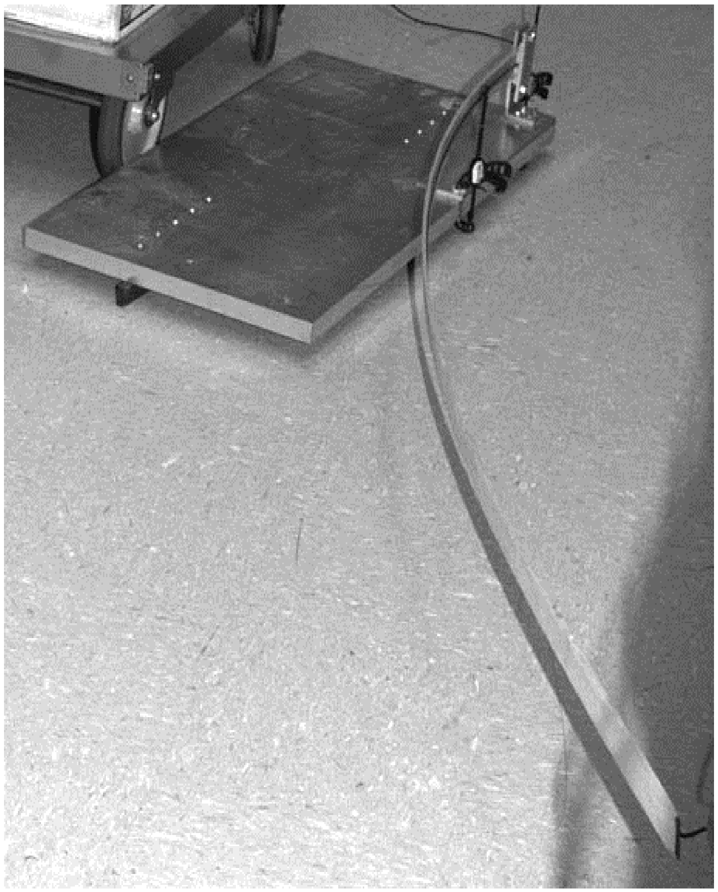

ETDR Signal Response of the Prototype Sensor

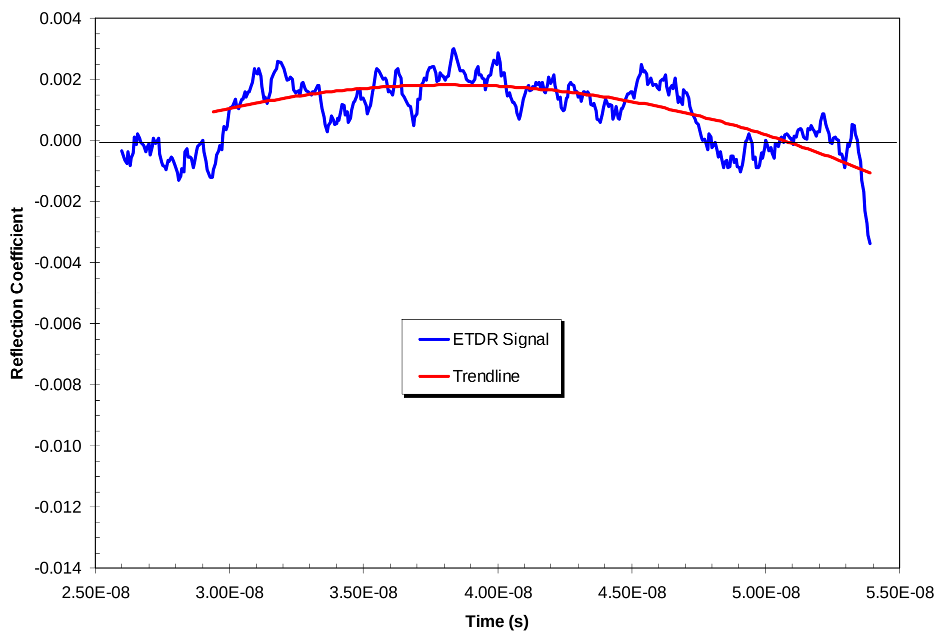

Shape Measurement of Large Structure (Cont.)

2nd Mode Reverse Bending

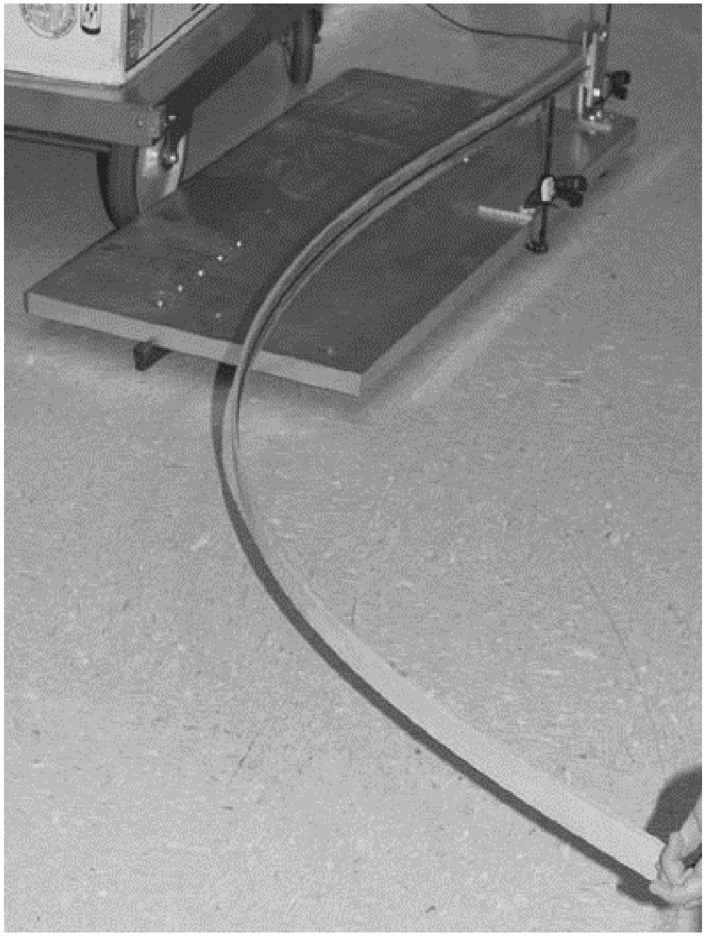

ETDR Signal Response of the Prototype Sensor

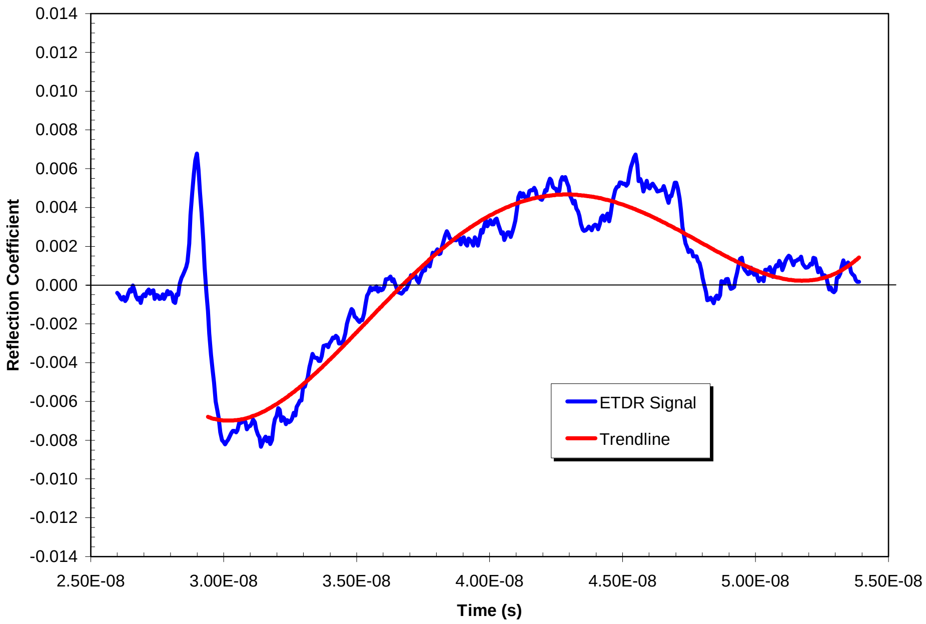

ETDR Film Sensor

ETDR Film Sensor

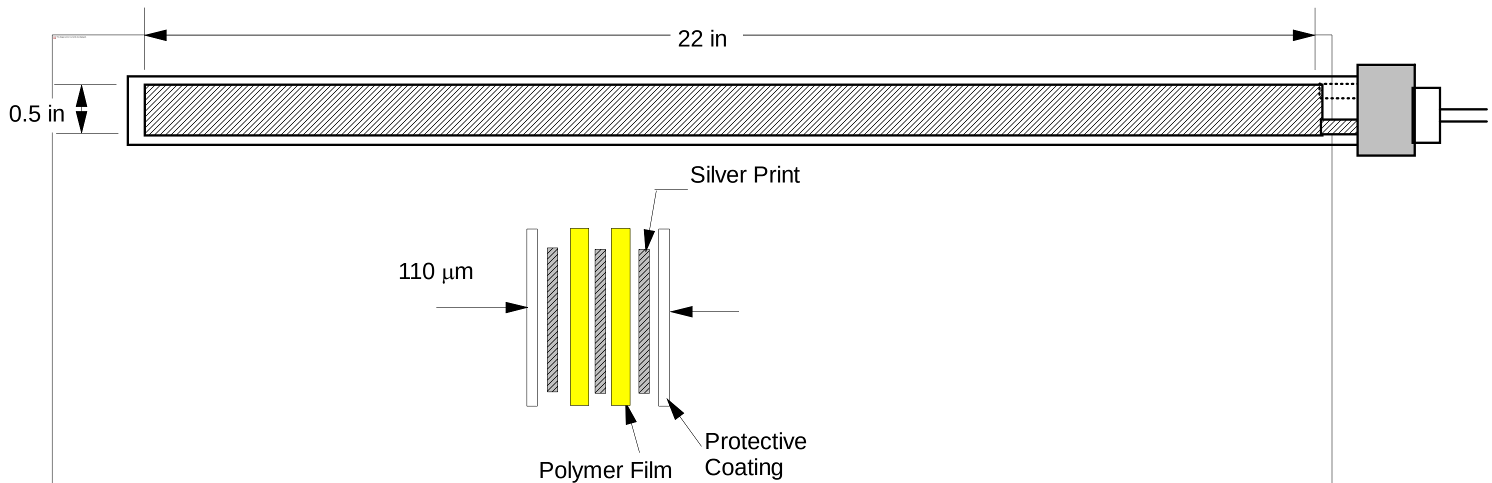

Envisioned Composite Laminate with Embedded ETDR Film Sensor

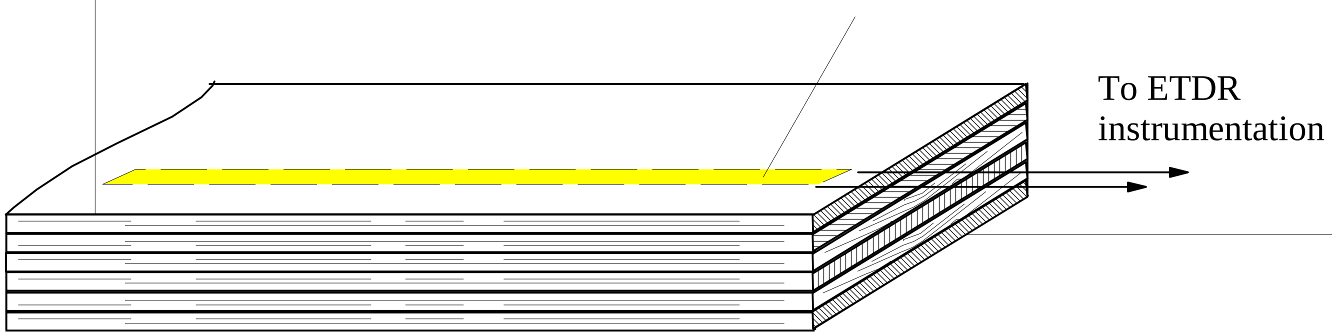

Laminated Composites

UAH

Impedance-Based Piezoelectric Sensor

Health Monitoring and Damage Detection

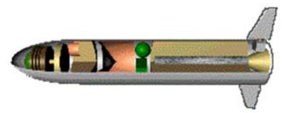

Go, No Go ?

- **Off-Duty Aircraft**
- **Stockpile Missile**

▶ **Need Active Sensor to Interrogate the Structure**

- **Bolted Structural Components**
- **Adhesively Bonded Substructures**
- **Riveted Substructures**
- **Composite Panels (Delamination)**
- **Engine Turbine Blades (Crack Damage)**

UAH

Piezoelectric Sensor

Piezoelectric Materials (Two-Way Fully Coupled Electromechanical Property)

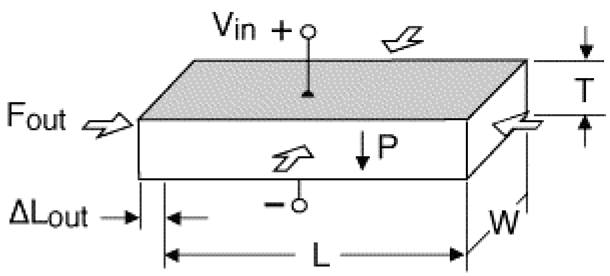

Piezo actuators convert voltage and charge to force and motion

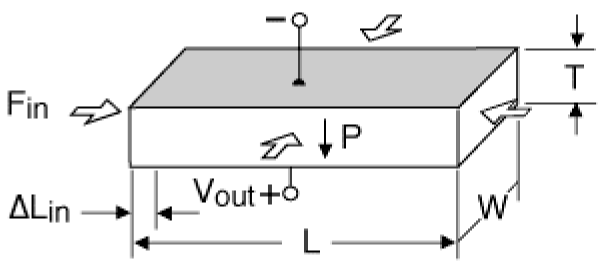

Piezo sensors convert force and motion to voltage and charge

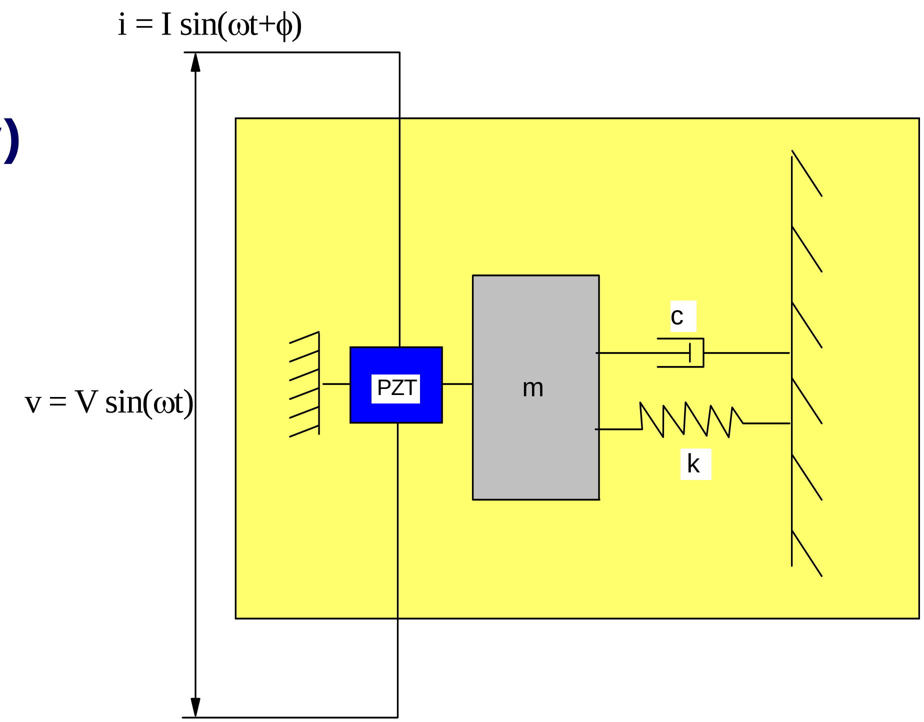

$$\text{Impedance} = \frac{(\text{Actuating Voltage})_{\text{in}}}{(\text{Sensing Current})_{\text{out}}} = \frac{v_{in}}{i_{out}}$$

UAH

Damage Detection Experiment

Bolt-Jointed Aluminum Cantilever Beam

Tight Joint: 1 N-m
Loose Joint: 0.1 N-m

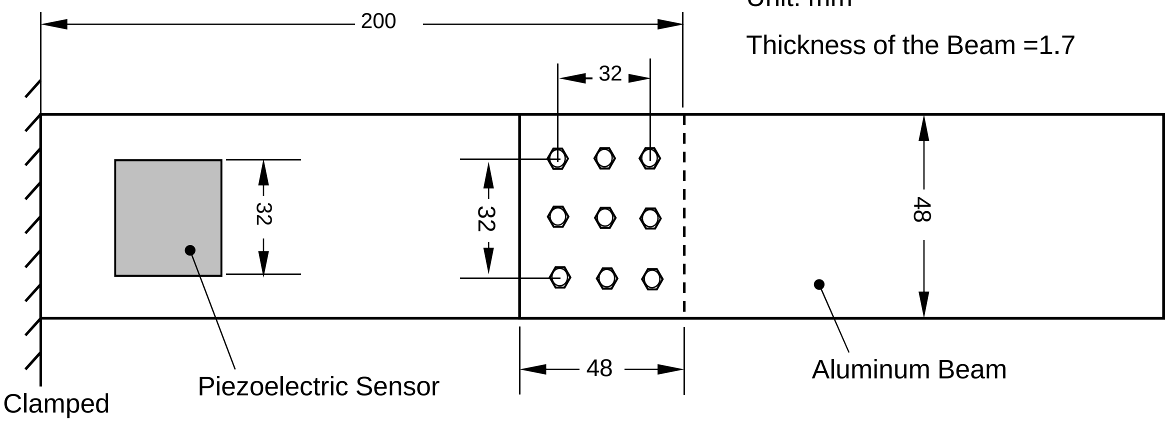

Experimental Set-Up

Experimental Results

Repeatability Test for “Healthy” Joint (All 9 Bolts were Tightened)

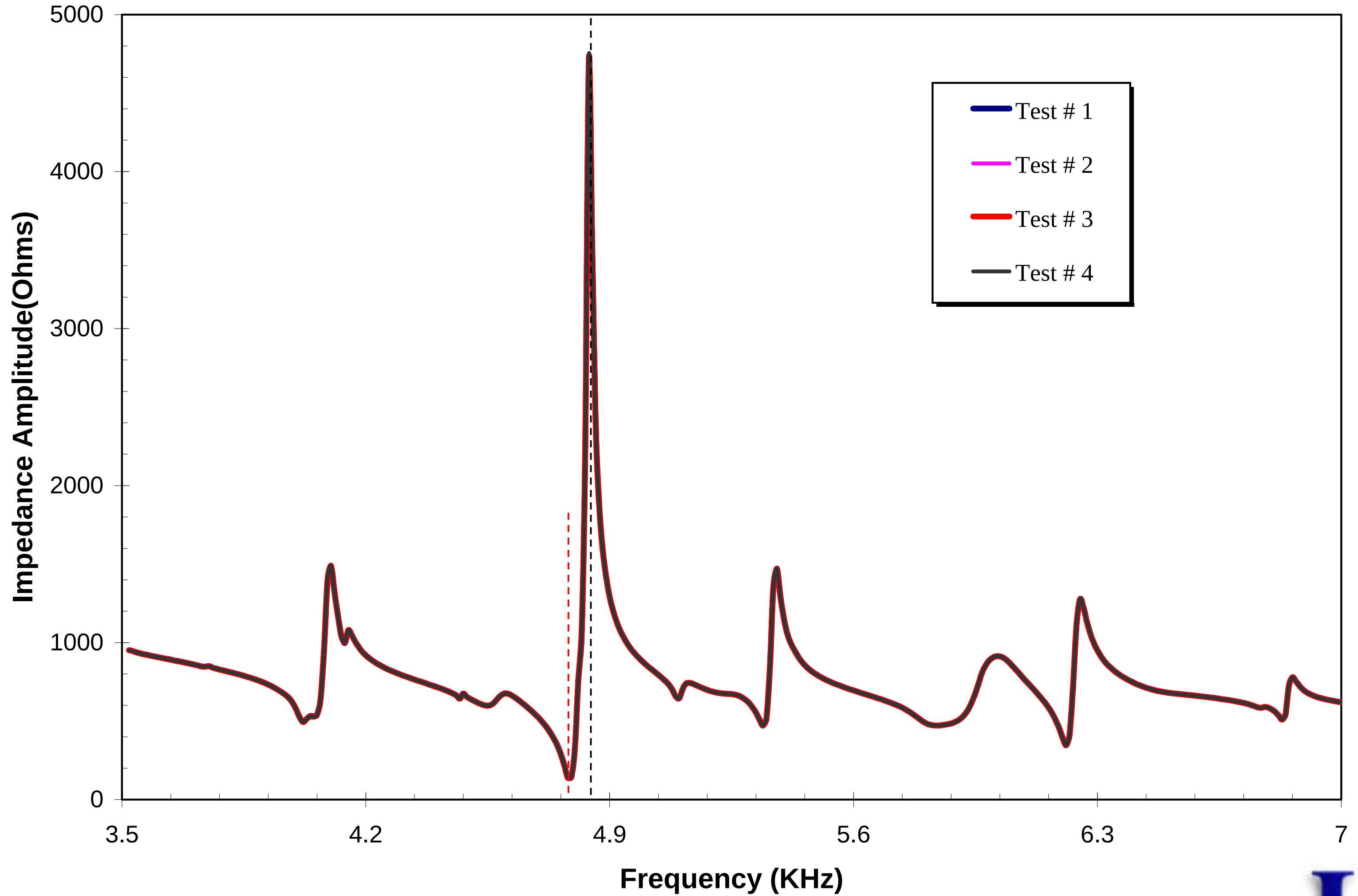

UAH

Experimental Results (cont.)

Repeatability Test for "Healthy Joint" Reference Baseline

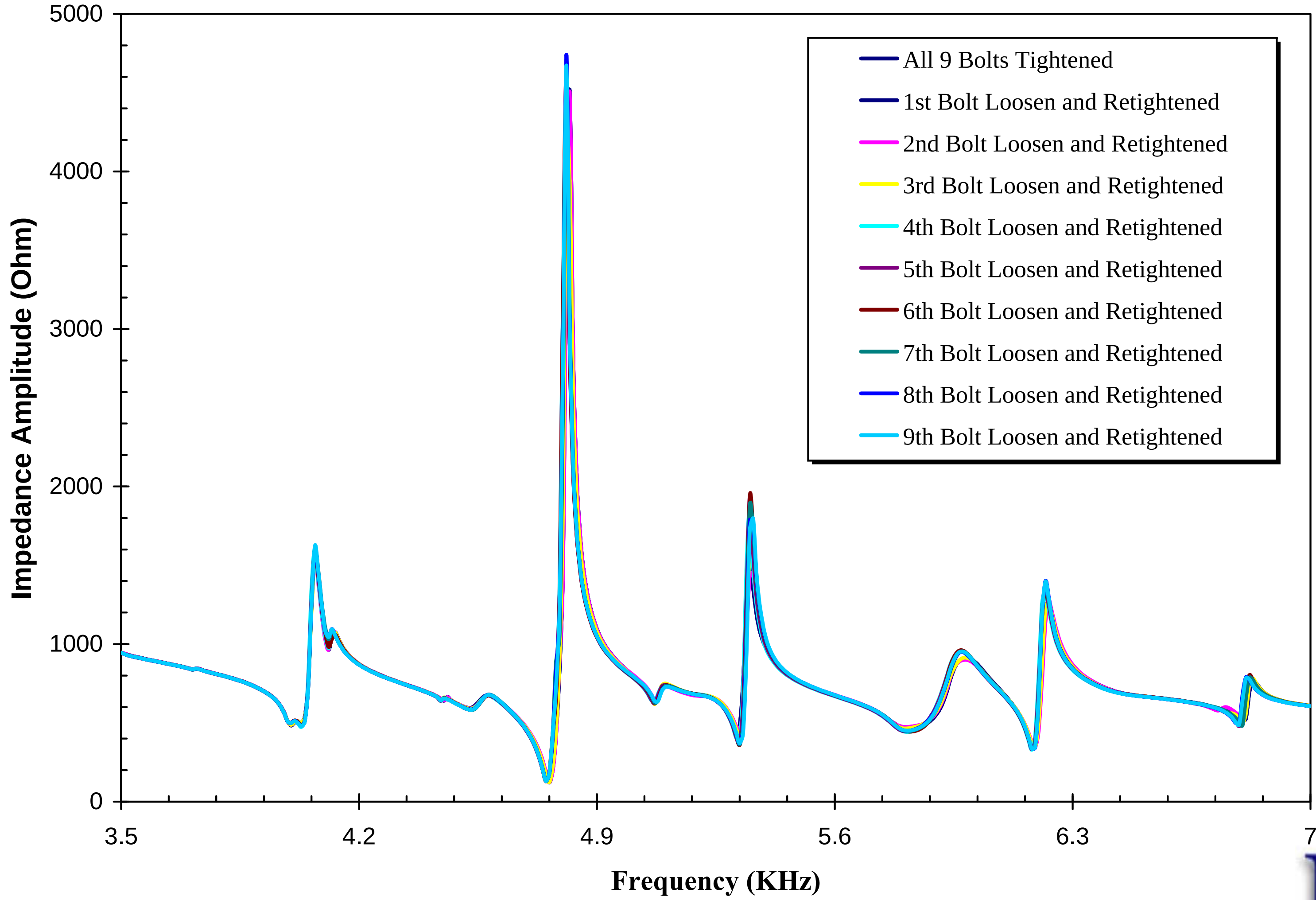

UAH

Experimental Results (cont.)

Damage Detection: 1st Bolt Loosen

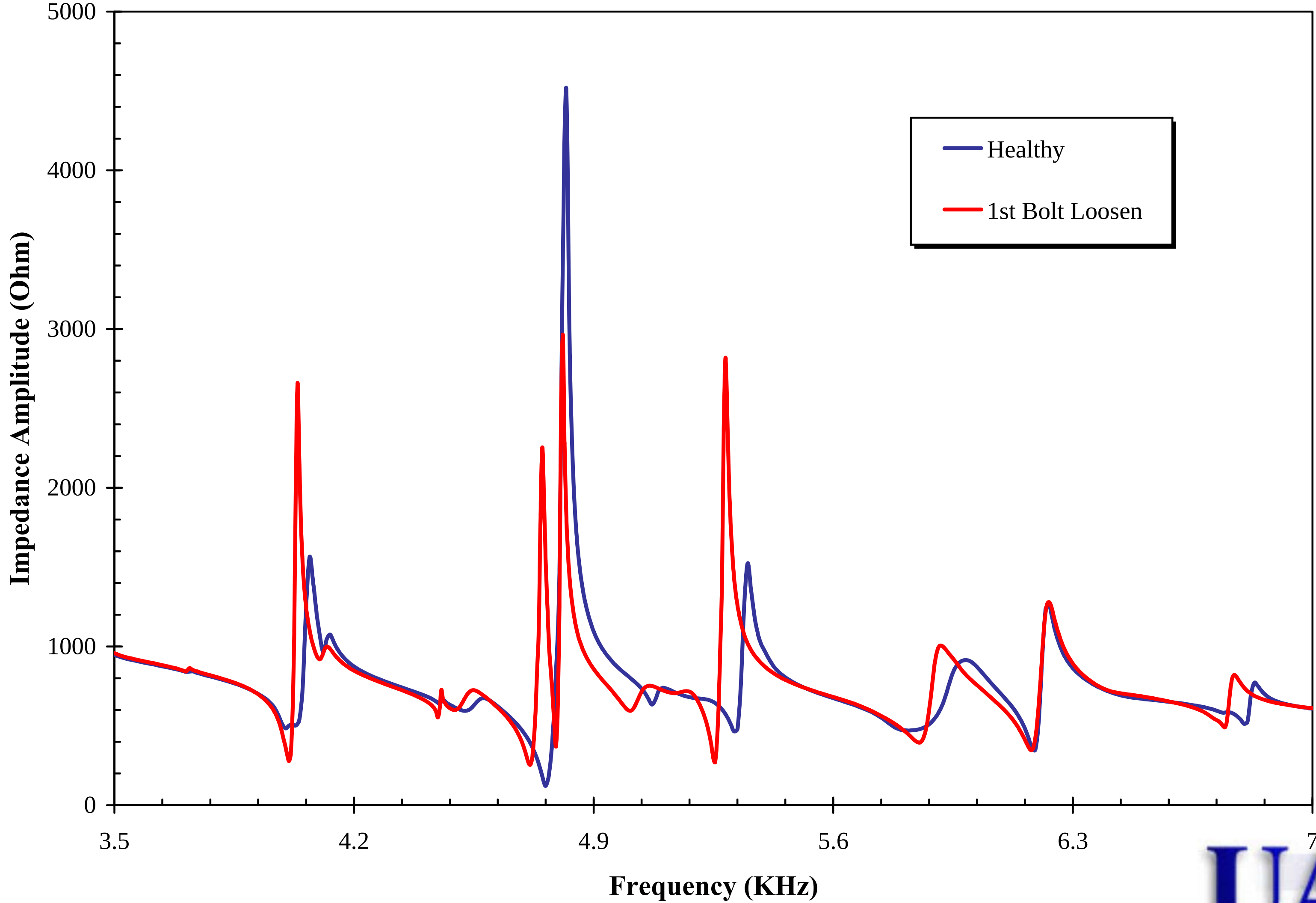

Experimental Results (cont.)

Damage Detection: 1st Bolt Loosen Repeated

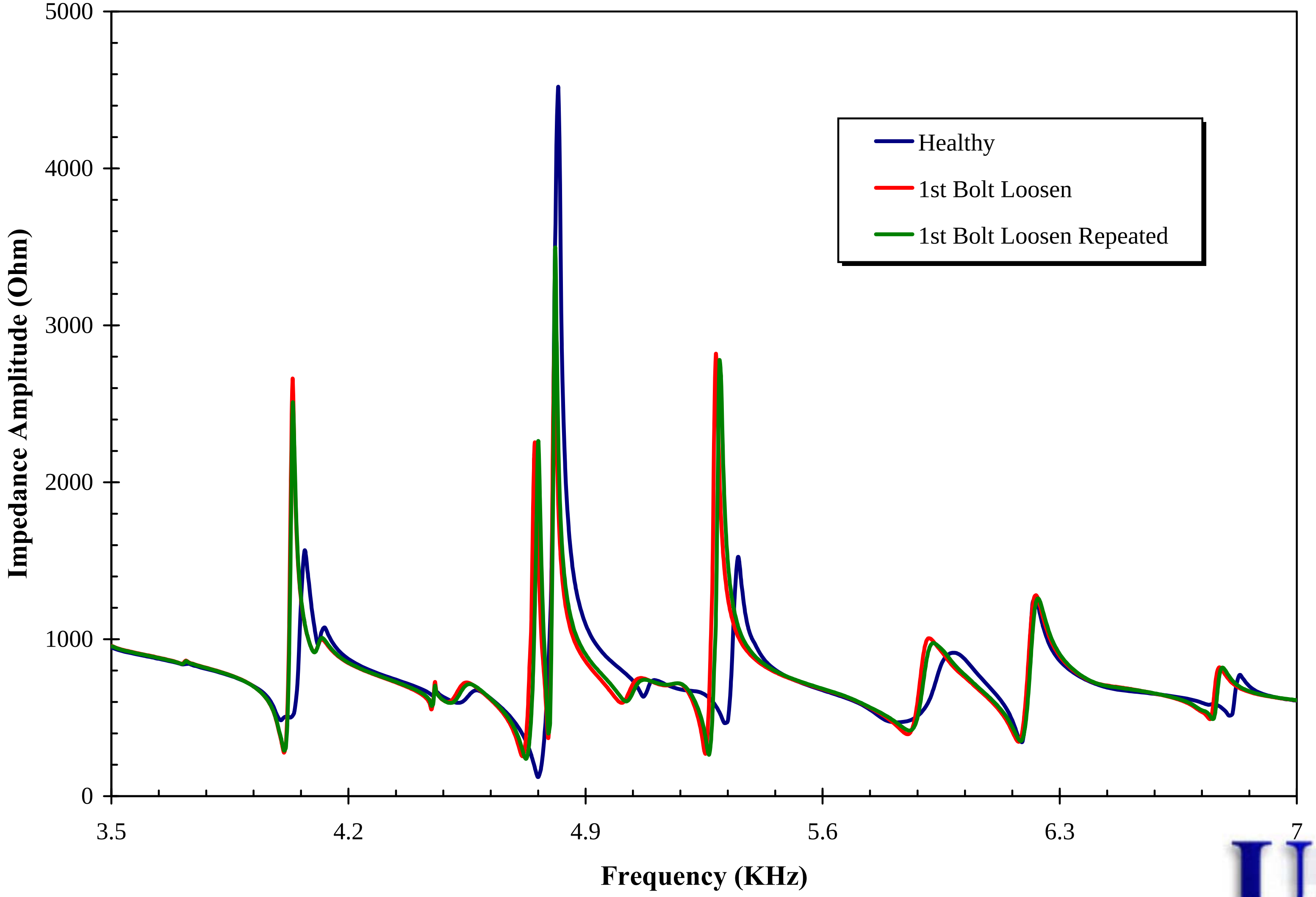

Experimental Results (cont.)

Damage Detection: with Increasing Number of Loose Bolts

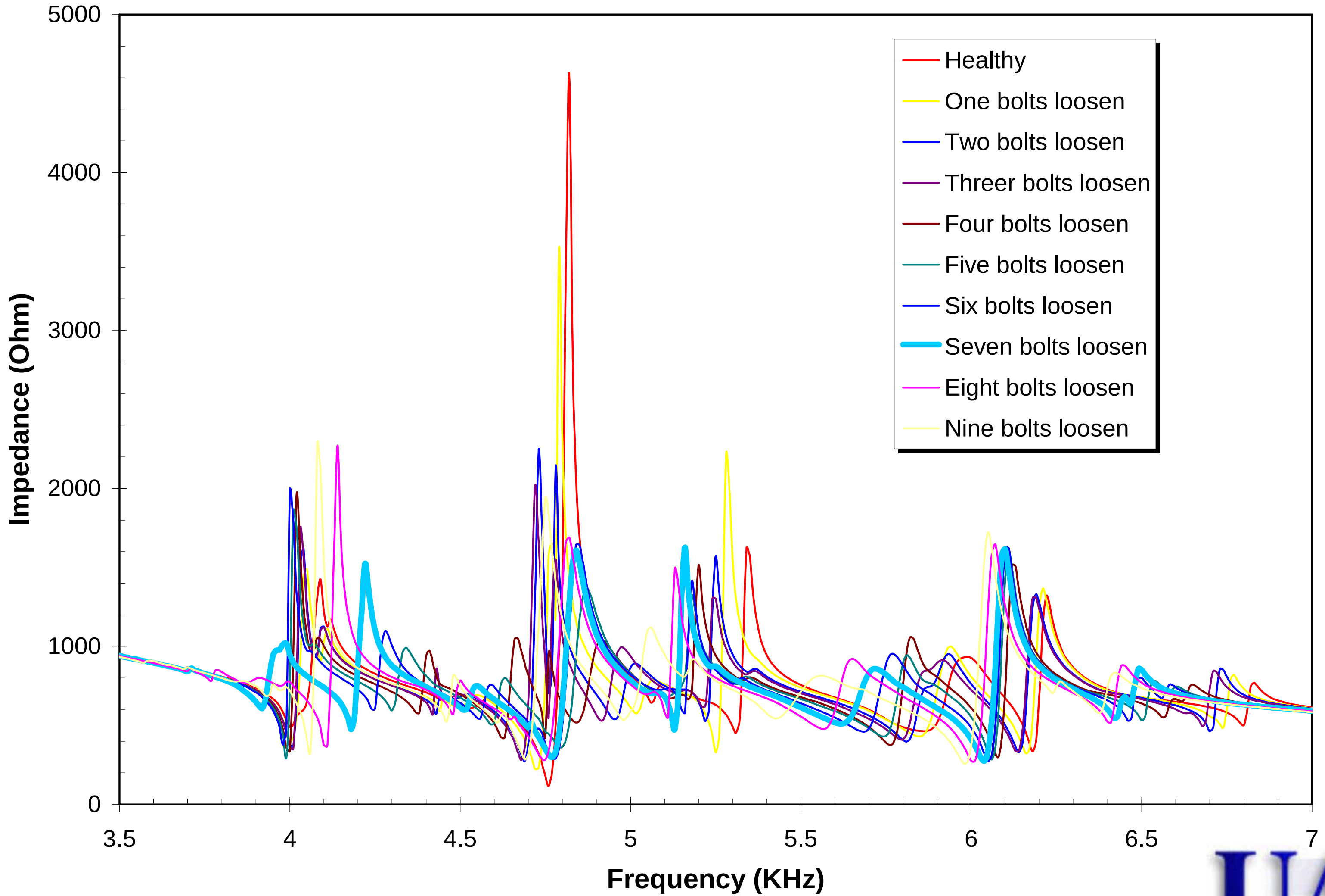

UAH

Experimental Results (cont.)

Frequency Variation on Even Numbered Modes

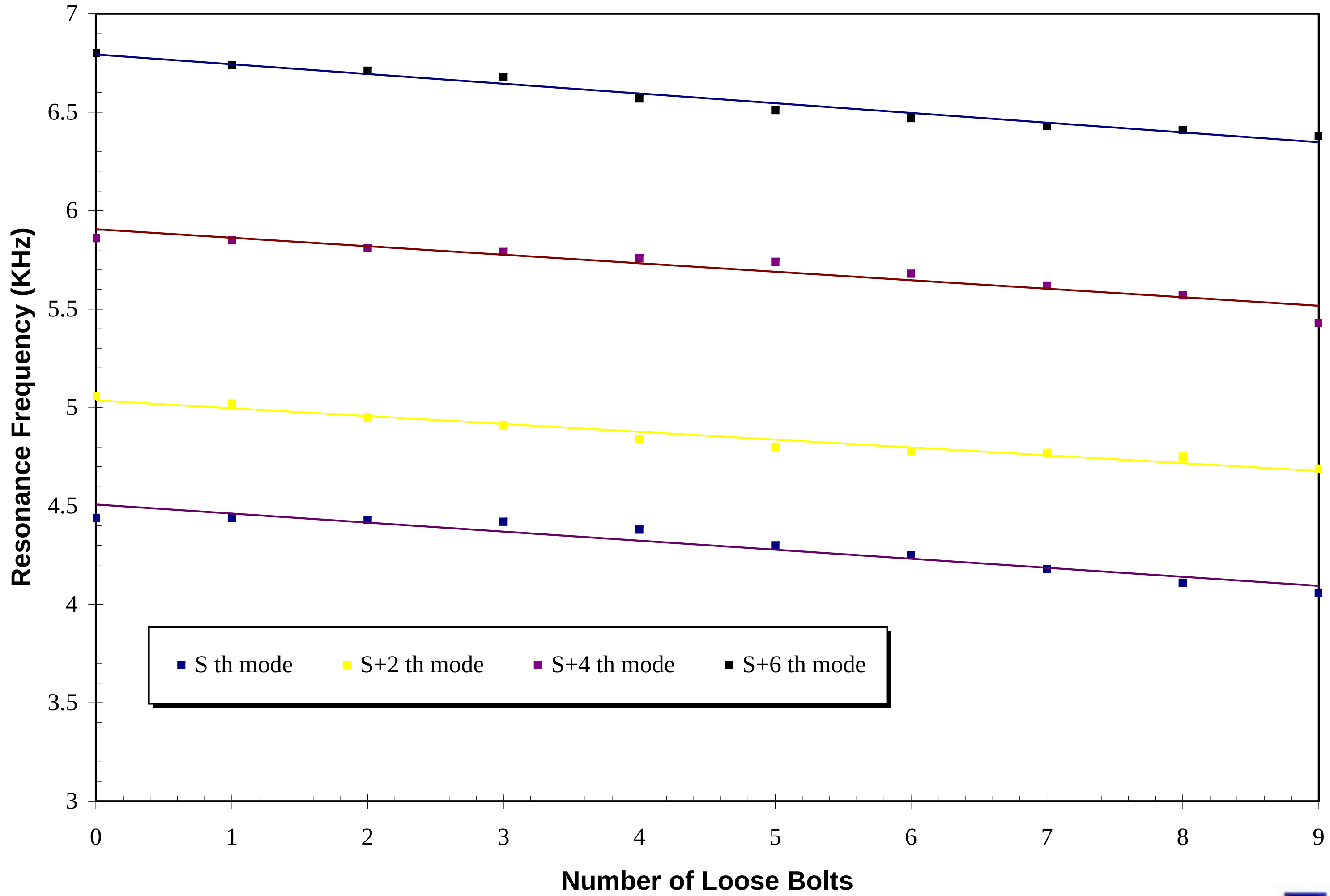

UAH

Finite Element Simulation

FE Model

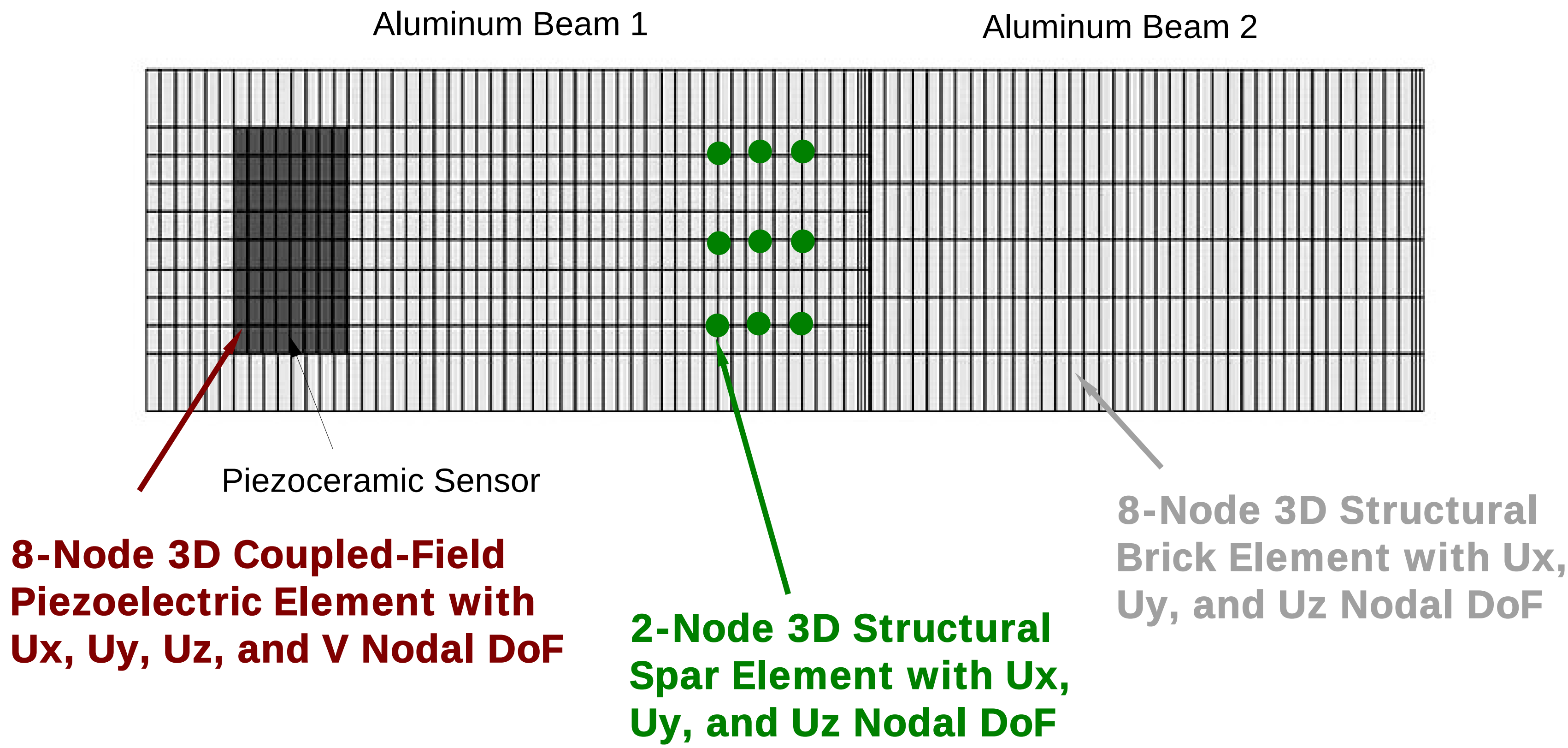

Harmonic Response Analysis -> Applied Load: Nodal Voltage, $V_o sin(\omega t)$
Output: Nodal Charge

Piezoelectric Constitutive Equation

$$\sigma_{ij} = D_{ijkl}\varepsilon_{kl} - e_{mij}E_m$$

$$q_i = e_{ijk}\varepsilon_{jk} + \mu_{ij}E_j$$

σ_{ij} = stress tensor

ε_{ij} = strain tensor

E_i = electric field vector

q_i = electric flux density vector

D_{ijkl} = elastic stiffness tensor (evaluated at constant electric field)

μ_{ij} = dielectric tensor (evaluated at constant mechanical strain)

$e_{ijk} = d_{ilm}D_{lmjk}$ = piezoelectric stress coefficient tensor

d_{ilm} = piezoelectric strain coefficient tensor.

FEA-Experiment Comparison

Impedance Spectrum of the Healthy Joint

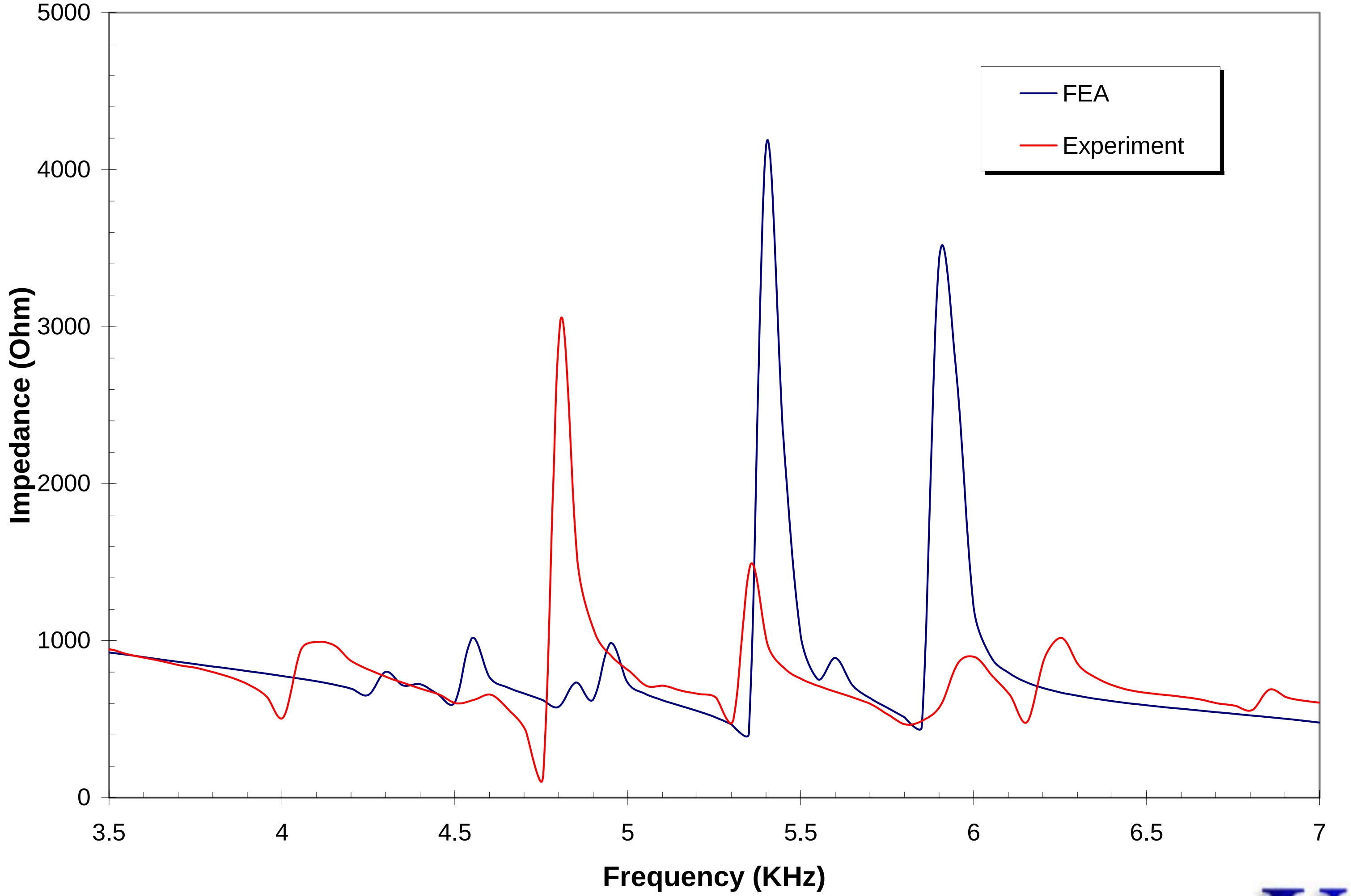

Hybrid Linear/Rotary Stepper Motor (Cont.)

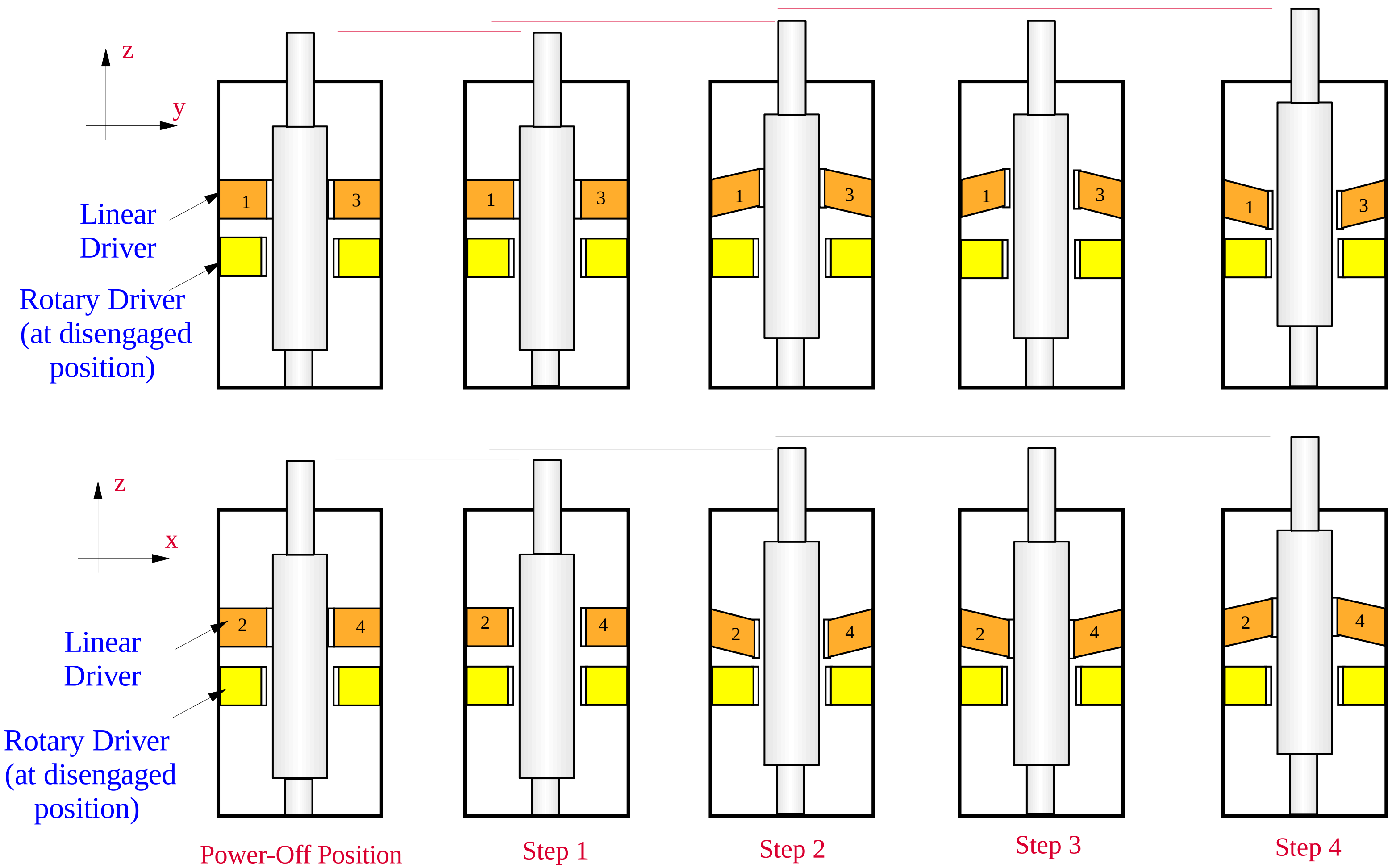

Hybrid Linear/Rotary Stepper Motor (Cont.)

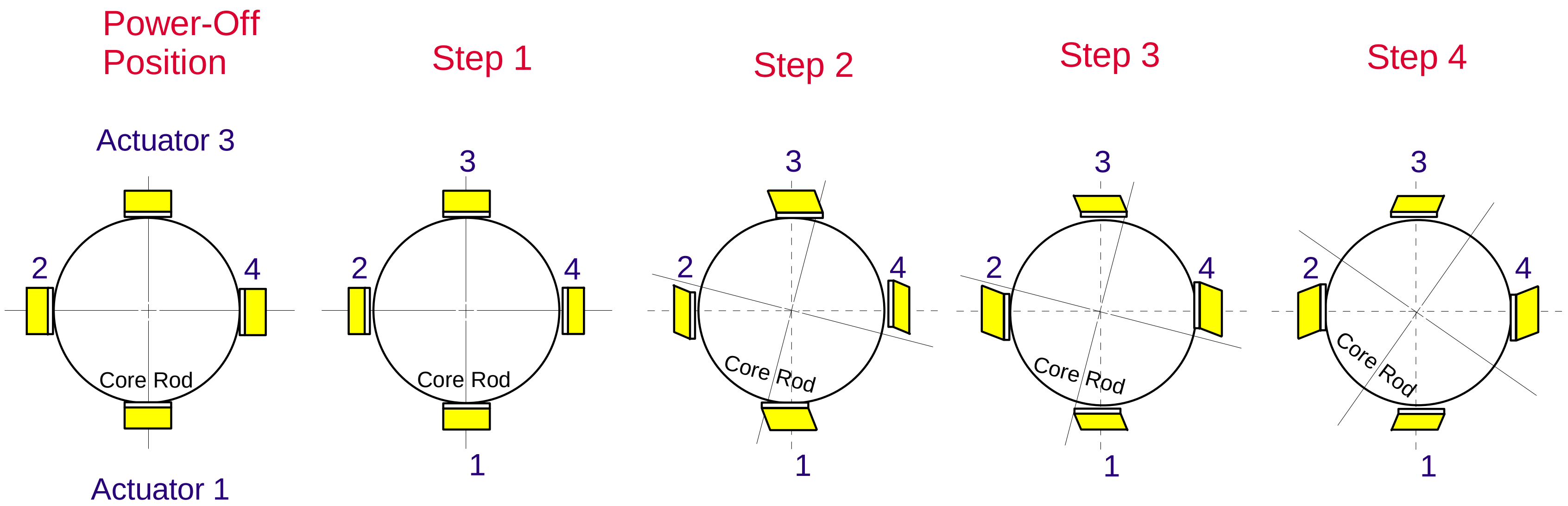

Concept Demonstration

Motor Assembly

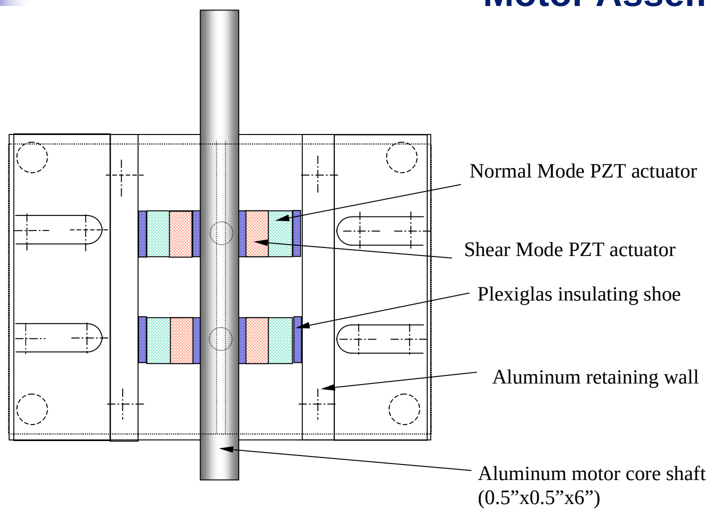

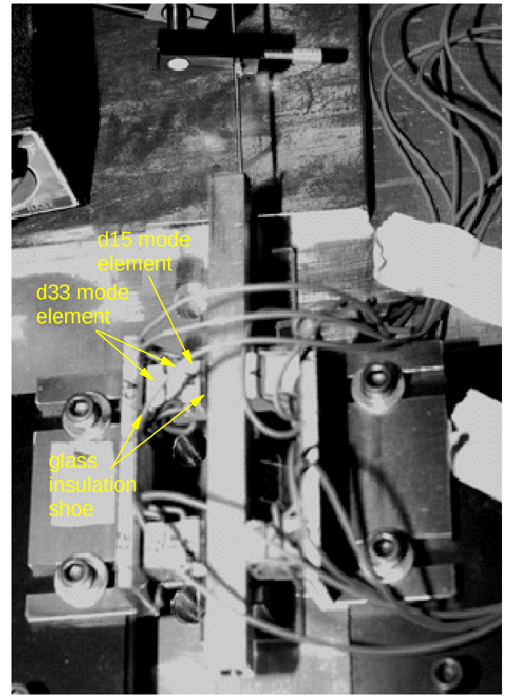

Driving Signal

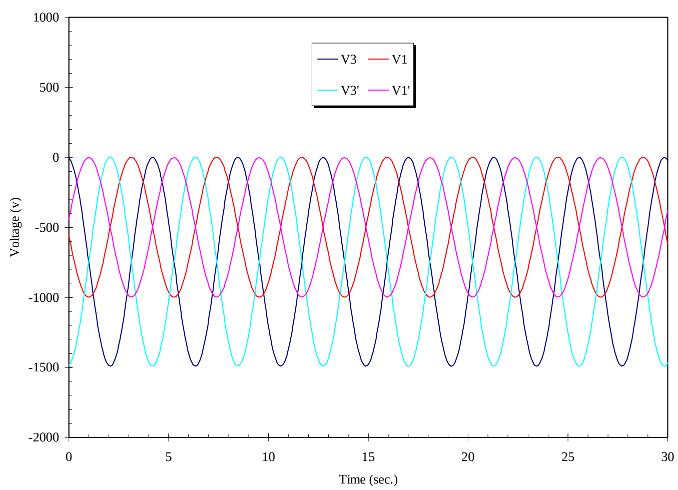

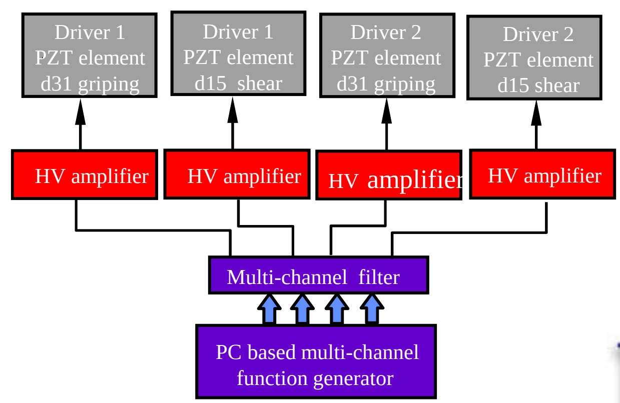

UAH

It Moved!

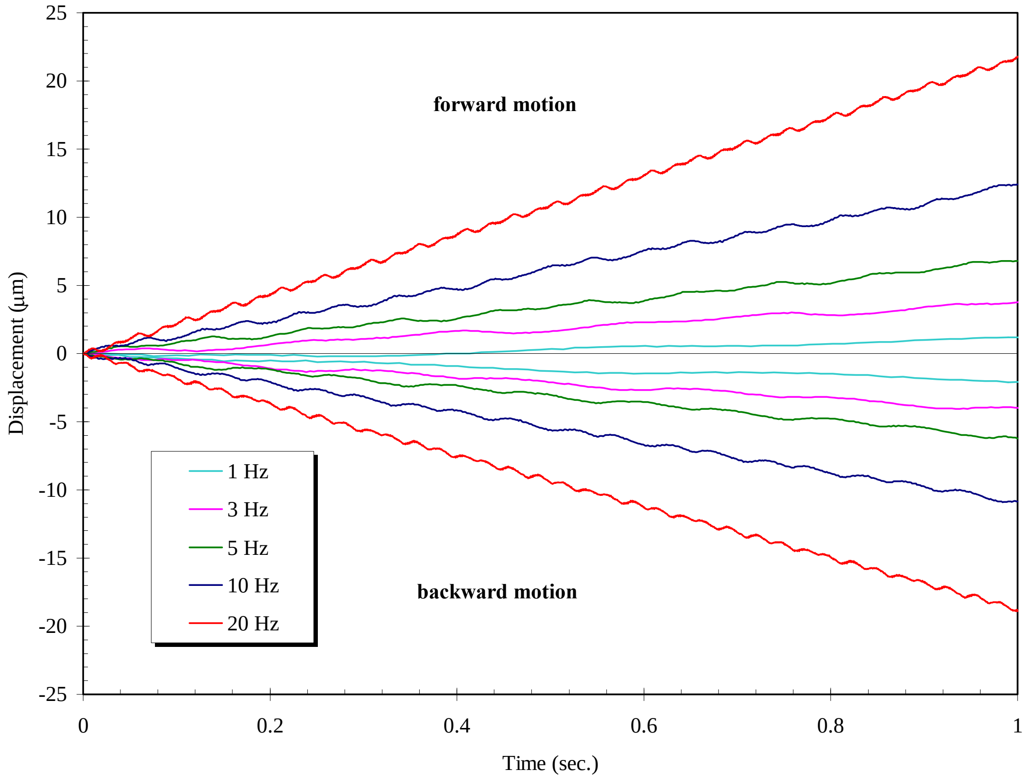

Driving Frequency (Hz)	1	3	5	10	20
Motor Core Velocity (µm/s)	1.2	3.8	6.8	12.4	21.8

Shape Memory Alloy (Nitinol) Actuator

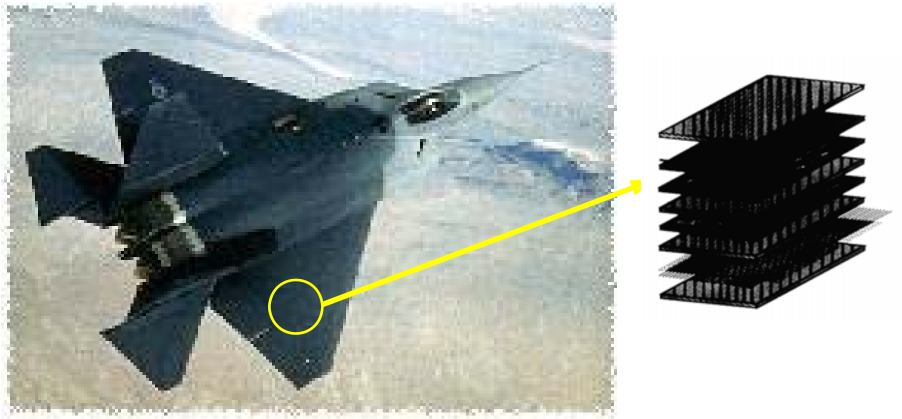

Shape Memory Alloy (SMA)

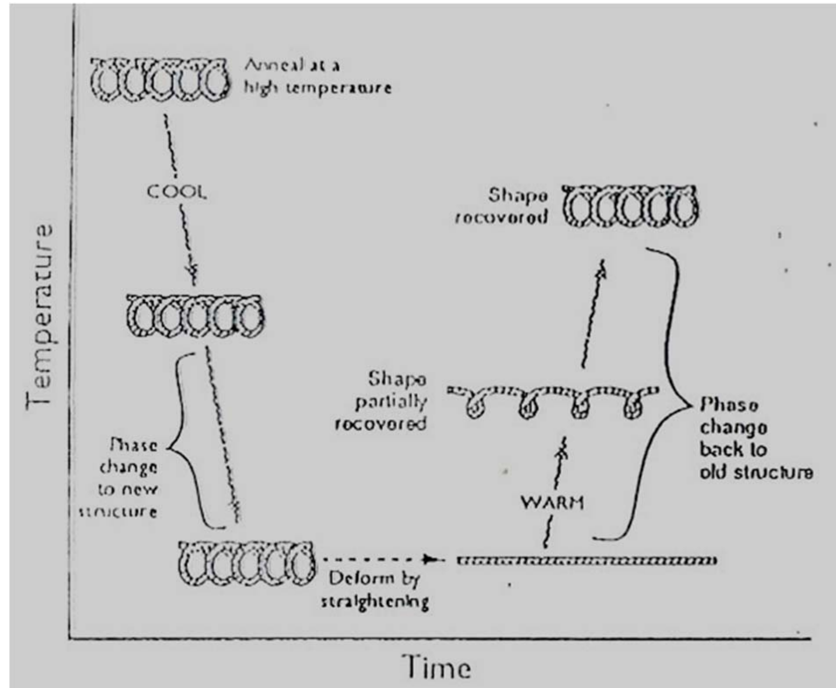

- **Variable Structural Stiffness for Natural Mode Tuning to Avoid Flutter**
- **Active Shape Control to Improve Aeroelastic Effectiveness**

Adaptive Stress Alleviation of Pressure Vessel

SMA Hybrid Composites Pressure Vessel

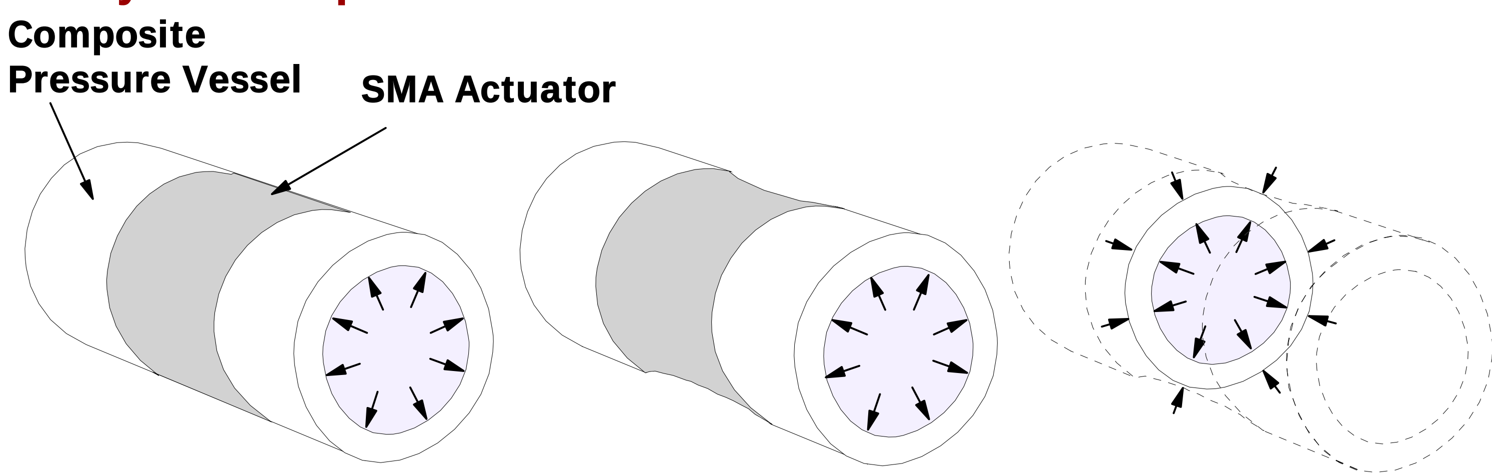

Composite cylinder with a layer of SMA actuator	**Activation of the SMA layer induces shrinkage against the cylinder**	**The induced pressure by the SMA layer creates the compound cylinder effect, resulting in structural stress alleviation on the composite cylinder**

Adaptive Stress Alleviation of Pressure Vessel

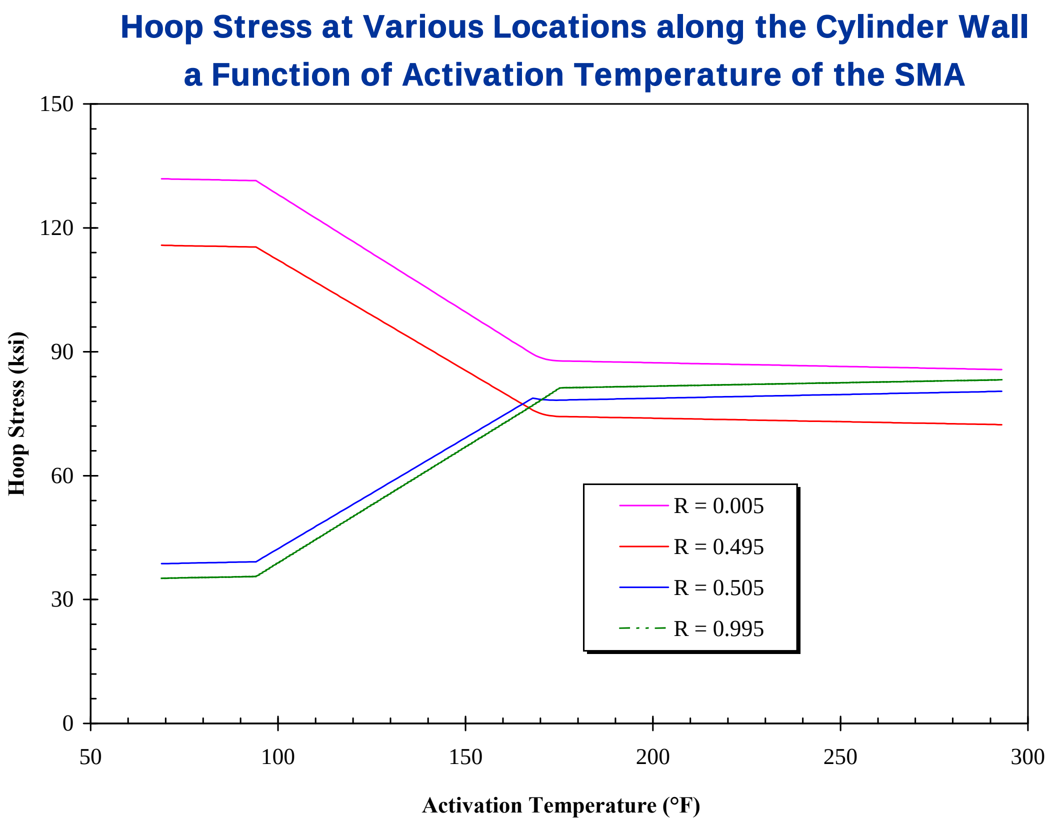

- **Significant stress alleviation can be achieved on a graphite/epoxy pressure vessel with a 1.5% recoverable prestrain of the SMA actuator**

Smart Materials & Structures

We cannot create life,

but can learn from life

to save life.

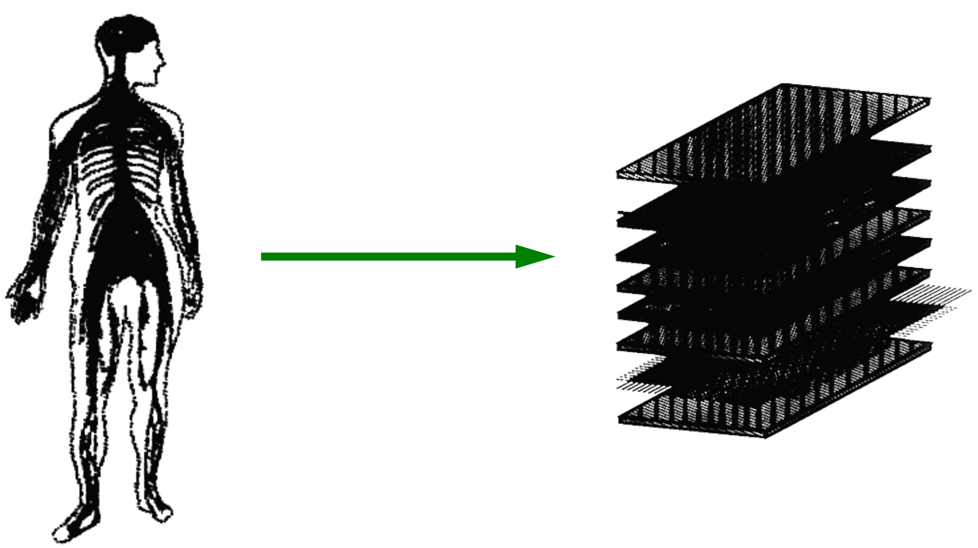

UAH

FEA of a Solar Sail Membrane

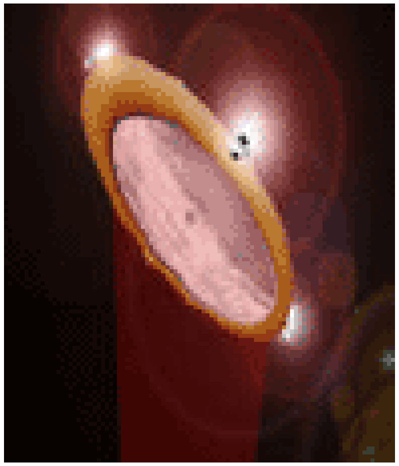

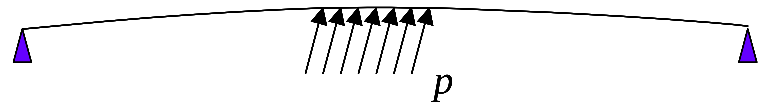

- circular membrane d = 10 m
- thickness = 7.6 microns
- partially illuminated light pressure with an oblique incident angle of 35°

Induced radial displacement contour

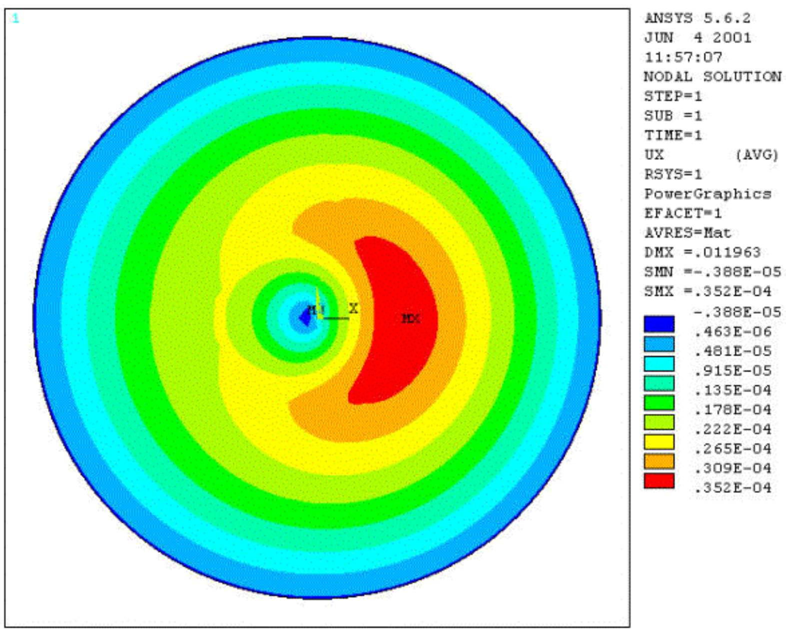

Induced radial stress contour

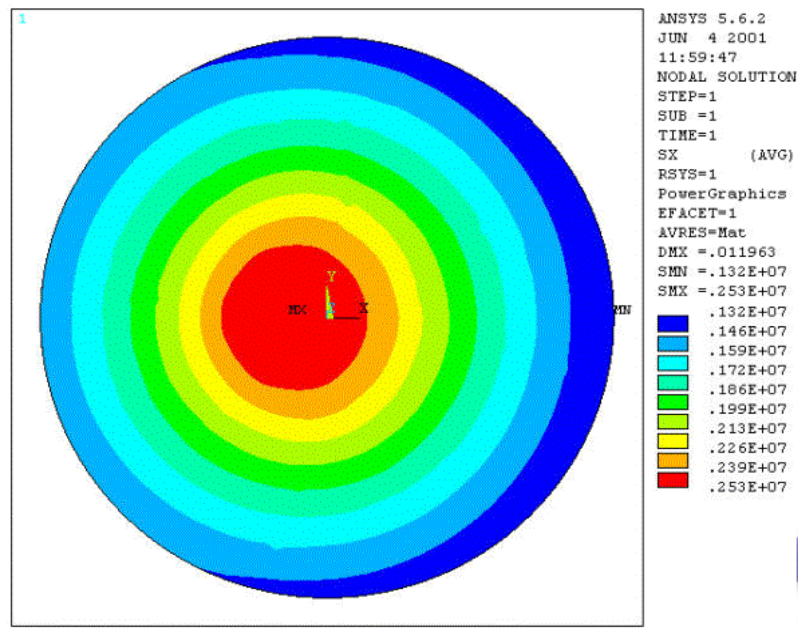

FEA Modeling of a Spindle Lug

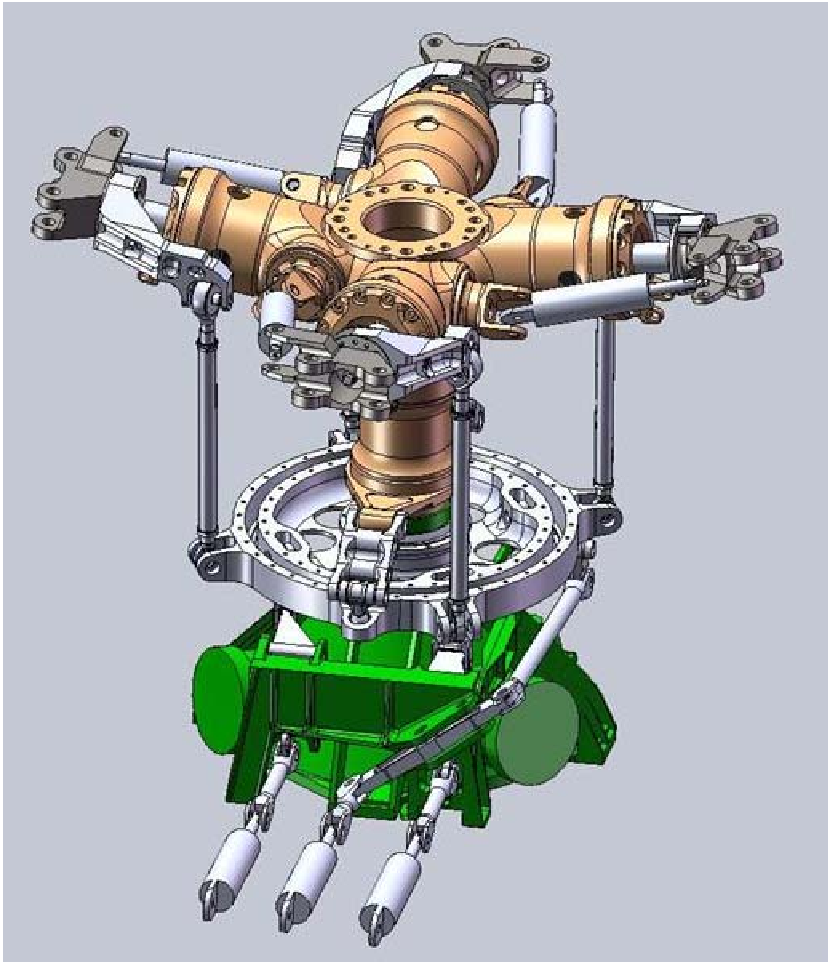

Background

- Crack failure occurred on the trailing lower lug
- Crack damage appears to initiate at the bushing/lug interface
- Fatigue and possibly fretting fatigue origins were SEM observed
- No root cause for the premature failure has been identified

FE Static Analysis

FEA Constraint and Load Conditions

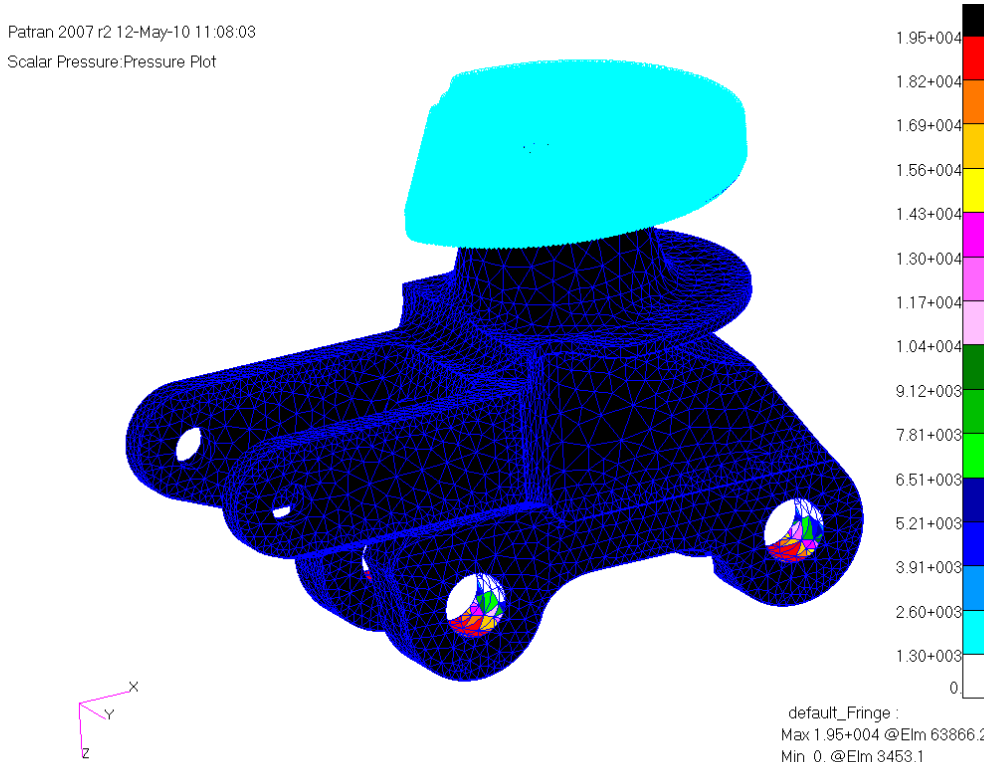

70,000 lbs total load applied

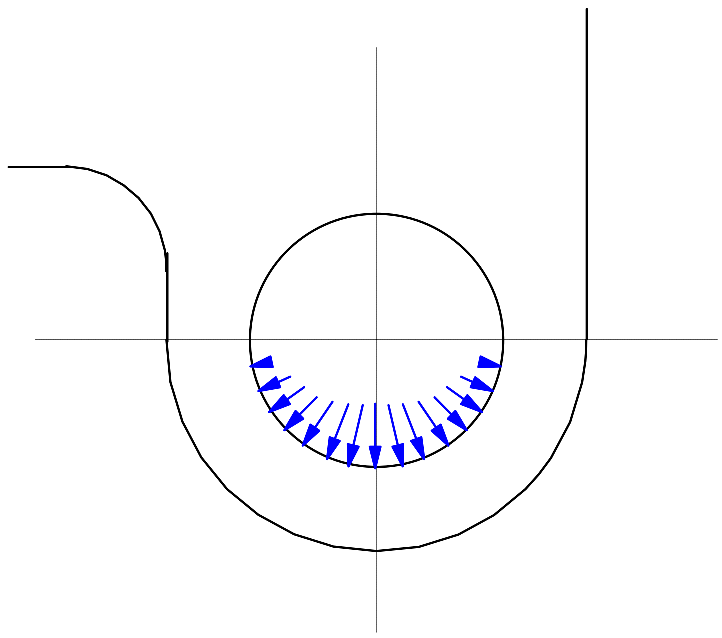

Surface Pressure

FEA Results

Tension Load = 29,000 lb , P = 3,200 psi

Principal Stress Contour

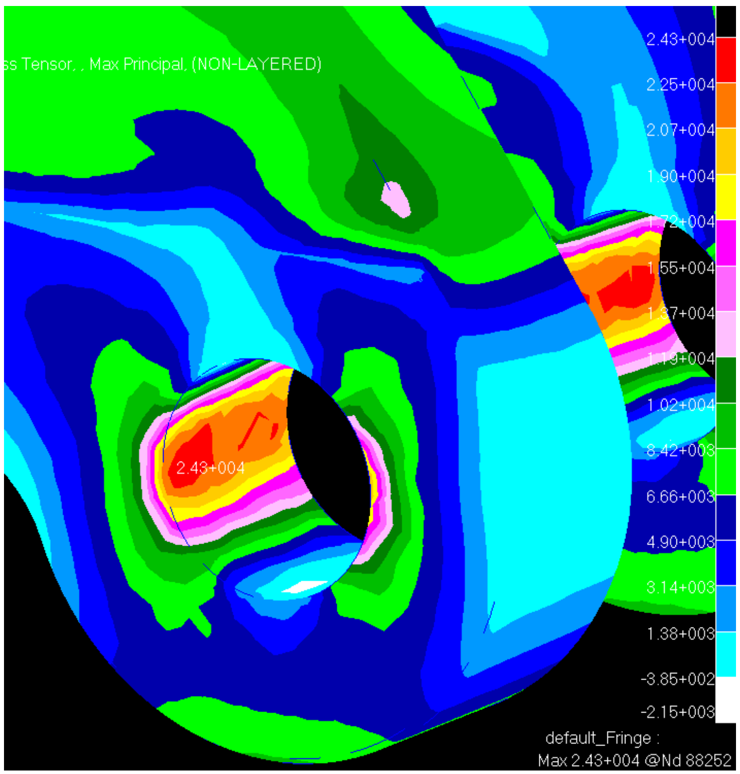

Von Mises Contour

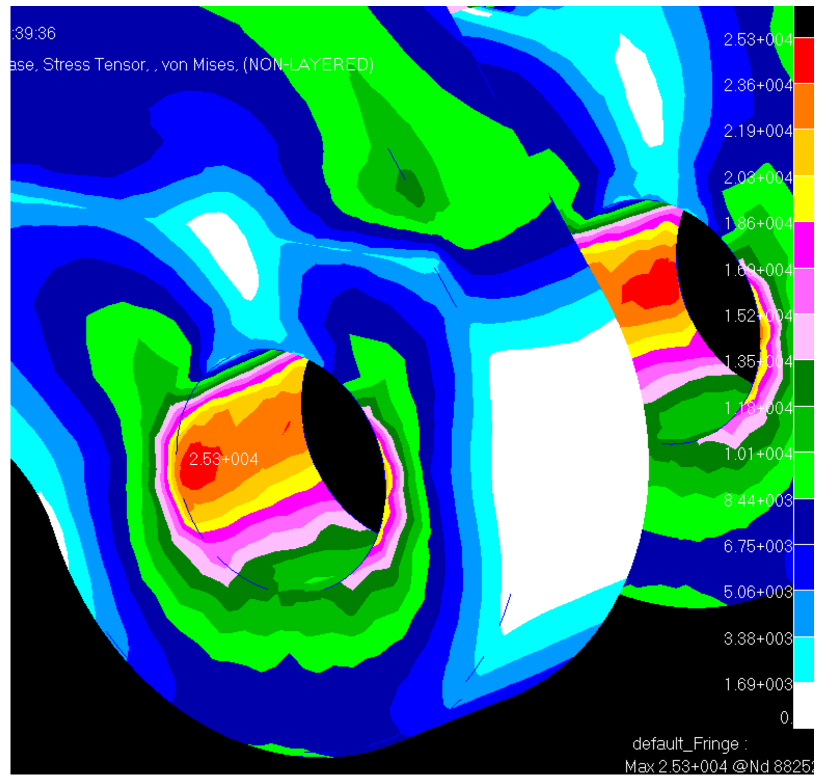

FEA Modeling of Hygro-Thermo-Mechanical Response of a Fiber Reinforced Polymer Composites Reinforcement

Unreinforced Masonry Wall with FRP Reinforcement Upgrade

Outdoor
(Changing Climate)

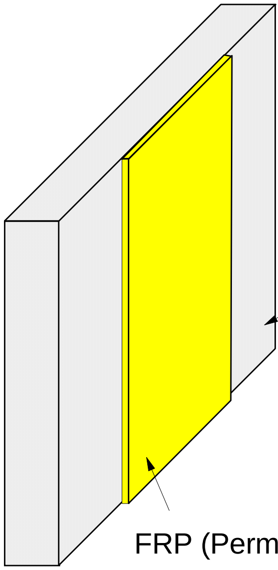

Indoor
(Controlled Climate)

Hygrothermal Stress and Moisture Damage at the Interface -> Delamination

UAH

Heat and Moisture Transport Model

$$\frac{\partial \theta}{\partial t} = \nabla \cdot (D_\theta \nabla \theta) + \nabla \cdot [\frac{\delta_P}{\mu} \nabla (hP_s)]$$

$$\rho c \frac{\partial T}{\partial t} = \nabla \cdot (\lambda \nabla T) + h_v \nabla \cdot [\frac{\delta_P}{\mu} \nabla (hP_s)]$$

ASTM version (2001)

h **= Relative humidity of the ambient air (dimensionless)**

μ **= Vapor resistivity of the media (dimensionless)**

δ_p **= Vapor permeability of the air (kg/m· s· Pa)**

P_s **= Saturation vapor pressure (Pa)**

All parameters are well defined and physically measurable.

UAH

Finite Element Modeling

- Finite element formulation in terms of nodal values

$$[C_e^*]\begin{Bmatrix}\dot{h}_e\\ \dot{T}_e\end{Bmatrix}+[D_e^*]\begin{Bmatrix}h_e\\ T_e\end{Bmatrix}=\{Q_e\}$$

where:

$\{N(x,y,z)\}$ = vector of shape functions

$\begin{Bmatrix}h_e\\ T_e\end{Bmatrix}$ = nodal humidty/temperature vector

$[D_e^*]=\int_V [B]^T[D^*][B]dV$ = element humidity and heat diffusion matrix

$[C_e^*]=\int_V \begin{bmatrix}C^* & 0\\ 0 & \rho c\end{bmatrix}\{N\}\{N\}^T dV$ = element humidity and heat capacity matrix

$\{Q_e\}=\int_S \{N\}q^* dS$ = element boundary humidity and heat flux

$[B]=\{L\}\{N\}^T$ $\quad$ $[D^*]=\begin{bmatrix}\overline{D}_h & \overline{D}_T\\ 0 & \lambda\end{bmatrix}$ = Humidity and heat diffusion matrix

- The Finite element formulation is implemented in FEMLAB computer software.

Case Study: Results

Transient relative humidity profile for T_{out}=40°C at T_{in}=20°C along the centerline at X=198 mm

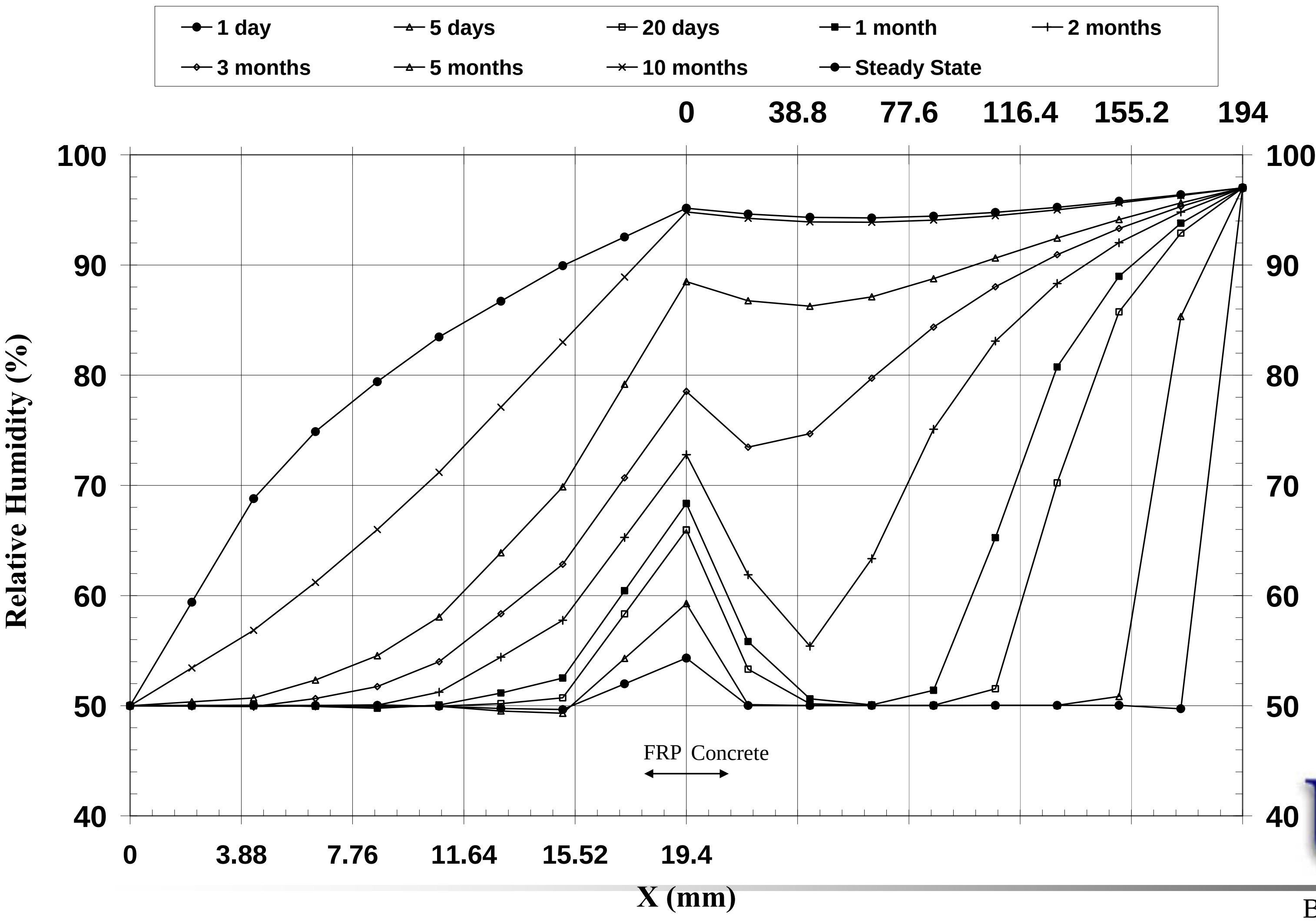

Hygro-Thermally Induced Interfacial Stresses

Finite Element Formulation

$$\{\sigma\} = [\overline{D}]\{\varepsilon_{elastic}\} = [\overline{D}]\{\varepsilon_{total} - \varepsilon_{swelling} - \varepsilon_{thermal}\}$$

$$\{\varepsilon_{thermal}\} = \{\alpha_1(T - T_{ref}) \quad \alpha_2(T - T_{ref}) \quad \alpha_3(T - T_{ref}) \quad 0 \quad 0 \quad 0\}^T$$

$$\{\varepsilon_{swelling}\} = \{\beta_1(\theta - \theta_{ref}) \quad \beta_2(\theta - \theta_{ref}) \quad \beta_3(\theta - \theta_{ref}) \quad 0 \quad 0 \quad 0\}^T$$

where:

α_i = the thermal expansion coefficients in the principle material directions $i = 1,2,3$

T_{ref} = the reference (strain-free) temperature

$$\{\varepsilon_{total}\} = \{\varepsilon_x \; \varepsilon_y \; \varepsilon_z \; \gamma_{xy} \; \gamma_{yz} \; \gamma_{xzz}\}^T = \{L\}\begin{Bmatrix} u \\ v \\ w \end{Bmatrix}$$

$$\{L\} = \begin{Bmatrix} \frac{\partial}{\partial x} & 0 & 0 & \frac{\partial}{\partial y} & 0 & \frac{\partial}{\partial z} \\ 0 & \frac{\partial}{\partial y} & 0 & \frac{\partial}{\partial x} & \frac{\partial}{\partial z} & 0 \\ 0 & 0 & \frac{\partial}{\partial z} & 0 & \frac{\partial}{\partial y} & \frac{\partial}{\partial x} \end{Bmatrix}^T$$

UAH

Finite Element Formulation

$$[K]\{U\} = \{F_B\} + \{F_S\} + \{F_{thermal}\} + \{F_{swelling}\}$$

where:

$\{U\} = \{u_1\ v_1\ w_1\ u_2\ v_2\ w_2\ \dots\ u_r\ v_r\ w_r\}^T$ = nodal displacement vector

$[K] = \int_V [B]^T [D][B] dV$ = element stiffness matrix

$\{F_B\} = \int_V [N]^T \{F_b\} dV$ = element body force vector

$F_S = \int_S [N]^T \{F_s\} dS$ = element force due to the surface loading

$\{F_{thermal}\} = \int_V [B]^T [D]\{\varepsilon_{thermal}\} dV$ = element force vector due to the thermal expansion

$\{F_{swelling}\} = \int_V [B]^T [D]\{\varepsilon_{swelling}\} dV$ = element force vector due to the moisture swelling

$[B] = \{L\}\{N\}^T$

$$\{N(x,y,z)\} = \begin{Bmatrix} N_1 & 0 & 0 & N_2 & 0 & 0 & . & . & . & N_r & 0 & 0 \\ 0 & N_1 & 0 & 0 & N_2 & 0 & . & . & . & 0 & N_r & 0 \\ 0 & 0 & N_1 & 0 & 0 & N_2 & . & . & . & 0 & 0 & N_r \end{Bmatrix}^T \text{ = shape function matrix}$$

- The Finite element formulation is implemented in FEMLAB computer software.

UAH

FEA Results

Interfacial shear stress, τ_{yz}, distribution for various outdoor temperatures along the z-axis at x = 198 mm in FRP laminate

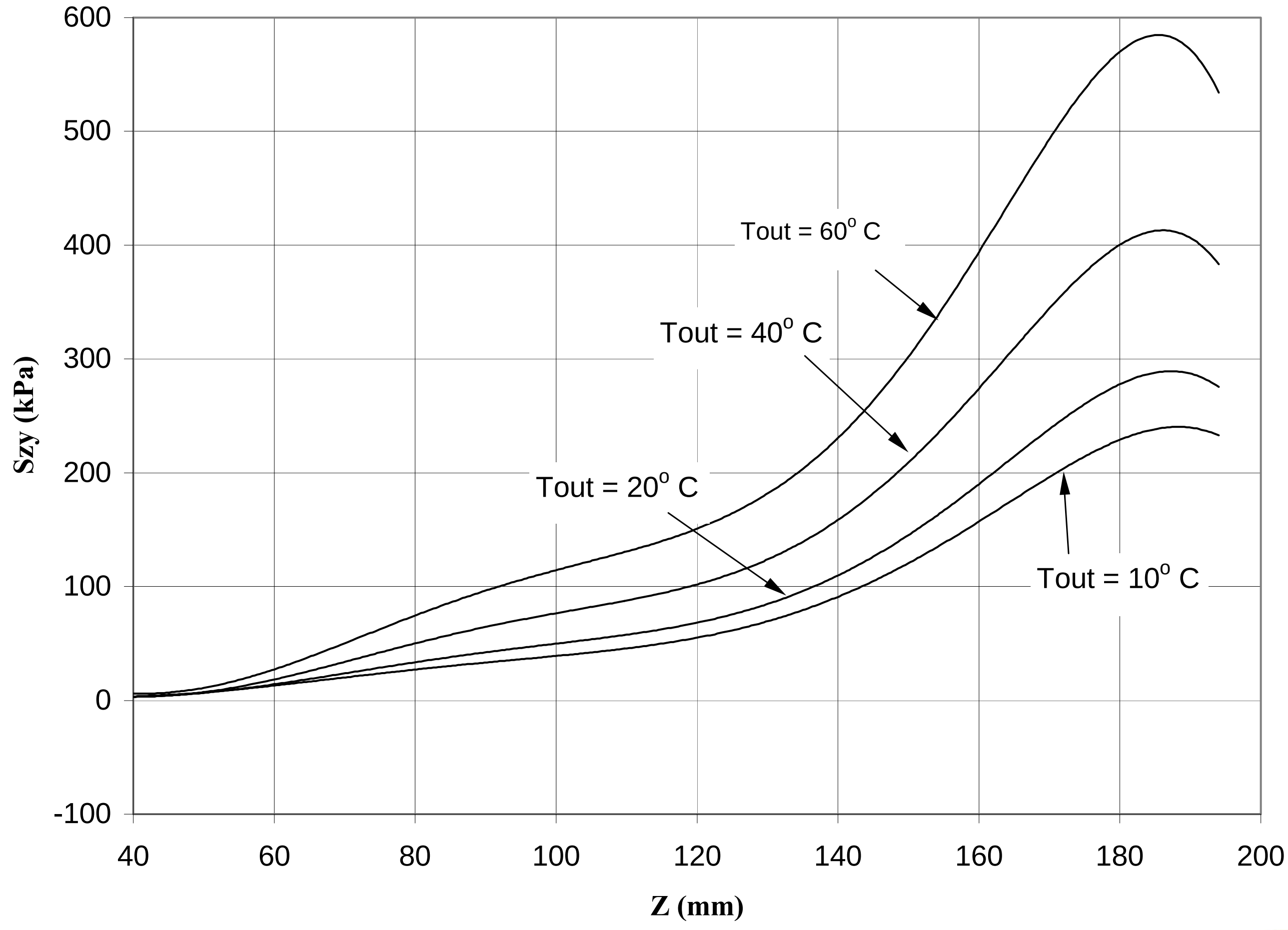

FEA Results (cont.)

Peeling stress, σ_y, distribution for various outdoor temperatures along the z-axis at x = 198 mm in FRP laminate